A Nondimensional Scaling Parameter for Predicting Pressure Wave Reflection in Stented Arteries

John J. Charonko, III

Thesis submitted to the faculty of the Virginia Polytechnic Institute and State University
in partial fulfillment of the requirements for the degree of

Master of Science
In
Engineering Mechanics

Pavlos Vlachos, Chair
Saad Ragab
Demetri Telionis

March 17, 2005
Blacksburg, Virginia

Keywords: coronary arteries, stents, fluid mechanics,
wave reflection, nondimesional parameters

A Nondimensional Scaling Parameter for Predicting Pressure Wave Reflection in Stented Arteries

John J. Charonko, III

ABSTRACT

Coronary stents have become a very popular treatment for cardiovascular disease, historically the leading cause of death in the United States. Stents, while successful in the short term, are subject to high failure rates (up to 24% in the first six months) due to wall regrowth and clotting, probably due to a combination of abnormal mechanical stresses and disruption of the arterial blood flow.

The goal of this research was to develop recommendations concerning ways in which stent design might be improved, focusing on the problem of pressure wave reflections. A one-dimensional finite-difference model was developed to predict these reflections, and effects of variations in stent and vessel properties were examined, including stent stiffness, length, and compliance transition region, as well as vessel radius and wall thickness. The model was solved using a combination of Weighted Essentially Non-Oscillatory (WENO) and Runge-Kutta methods. Over 100 cases were tested. Results showed that reasonable variations in these parameters could induce changes in reflection magnitude of up to ±50%. It was also discovered that the relationship between each of these properties and the resulting wave reflection could be described simply, and the effect of all of them together could in fact be encompassed by a single non-dimensional parameter. This parameter was titled “Stent Authority,” and several variations were proposed. It is believed this parameter is a novel way of relating the energy imposed upon the arterial wall by the stent, to the fraction of the incident pressure energy which is reflected from the stented region.

Acknowledgements

First, I would like to thank my committee for their help and support over the last few years. In particular I would like to thank Dr. Vlachos for his support and encouragement, and for first getting me involved in real research during the senior year of my Bachelor's degree. Dr. Ragab deserves recognition for his exceptional patience, and for all the assistance he has given me in developing the numerical model upon which this research is based. Finally, Dr. Telionis deserves thanks for his role as Devil's advocate. His "discussions" about fluid mechanics with Dr. Vlachos have probably been among the most educational experiences I have had at Virginia Tech. It has been exciting working with all of them.

I would also like to thank all of other graduate students, past and present, who have worked with me over the length of this project. You helped keep my time here entertaining and worthwhile. Your assistance is deeply appreciated.

Finally, I would like to thank my parents, without whom I would not be the person I am today. The love and support they have shown me throughout my life has been incredible, and they have always had the wisdom to know when I still needed a helping hand, and when they should step back and let me succeed or fail on my own. For everything you have done for me, my thanks, and my love.

Table of Contents

List of Figures

List of Tables

List of Symbols

A = lumen area of vessel
A_0 = some reference area, typically diastolic area
b = an empirically determined fitting constant used in the stent authority relation
D = bending stiffness coefficient
E = modulus of elasticity
E_0 = modulus of elasticity of the vessel wall
E_1 = maximum modulus of elasticity of the stent
f = pulse frequency, or heart rate
F = list of dependent variables, functions of dependent variables q
h = vessel wall thickness
L = total length of the stent, including transition regions
P = fluid pressure
P_0 = some reference pressure, typically minimum diastolic pressure
ΔP = pulse pressure, the difference in pressure between diastole and systole
q = list of independent variables
r = inner radius of vessel
r_0 = some reference radius, typically maximum inner radius at systole
t = time
u = flow velocity in the x-direction
w = inward deflection of vessel wall from rest
x = distance along the x-direction

β = coefficient relating pressure and area
δ = length of the compliance transition region
υ = Poisson's ratio
ρ = fluid density

SA = stent authority
TSA = total stent authority
GSA = geometric stent authority

List of Equations

A Nondimensional Scaling Parameter for Predicting Pressure Wave Reflection in Stented Arteries

Introduction

Cardiovascular disease has historically been the leading cause of death in the United States [1], and accounts for approximately one third of all deaths worldwide [2]. In the US, coronary artery disease in particular accounts for over fifty percent of these deaths, and in 2004 was the single largest killer [1]. As a result, investigation into the causes of and treatments for this disease has become a high priority among researchers. Arterial stenoses, one common form of coronary artery disease, are of great importance since they can result in an interruption in blood flow to the heart; common causes are the build up of plaque within arteries or the thickening of the arterial wall. Intravascular stents are a type of implanted prosthetic device that has received increasing acceptance among the medical community for the treatment of these problems. Inherently, stent implantation alters the mechanical environment of the vessel introducing a complicated strongly coupled fluid solid interaction. Despite the wide use of stents, our understanding of the associated governing mechanics is still lacking. This paper addresses a new method for predicting the performance of an intravascular stent based on the interaction between the fluid and mechanical properties of the system.

Stents, while successful in the short term, are subject to high failure rates due to restenosis and thrombosis. In one study, Knight et al. [5] found that in patients receiving a balloon angioplasty and subsequent stenting, restenosis resulted in a 24% failure rate for the procedure over a six month span, better than angioplasty alone (53%), but still leaving much room for improvement. It is believed that the high failure rates are partly due to abnormal wall stresses [6, 7, 8], and disruption of the flow around the stent [9, 10, 11, 12] which can be caused by both irregular geometry and compliance mismatch between the stent and the artery. Although progress in suppressing acute stent failure has been made using drug-eluting stents [13, 14, 15], this technique does not address the underlying mechanical and fluidic disruption. Despite their problems, stents are currently the most effective treatment for many types of coronary artery disease, and research shows that stent design remains an important factor in the long-term success of the implant [15, 16, 17, 18, 19, 20]. Therefore, pursuit of improvements in stent design is of great importance. As of yet, analytical models remain simplistic, and innovations have resulted mainly from experimental observations or trial-and-error clinical studies.

One major weakness of many computational approaches was that they examined only the mechanics of the walls or stent. Chua et al. [21] used LS-DYNA and ANSYS to study the initial expansion of a realistic stent model under varying inflation pressures, focusing on differences in strut stresses and final stent geometry. However, their analysis omitted any consideration of the effect of the vessel walls, and did not examine the coupling of the mechanical system to the fluid pressure after implantation.

Petrini et al. [22] developed finite element models of two commercial stents and examined their behavior when expanded into curved vessels. They were able to successfully predict the rotational moments required to generate a given angle of curvature, as well as predict the mechanical stresses within the stent, but their analysis neglected the contribution of the walls and the delivery catheter.

Other researchers have focused on the behavior of the blood flow within the system, considering only the geometry of the stent and wall, and not their coupled motion. To keep the simulations manageable, approximations such as restricted domains, steady flow, and simplified geometries are also common in many studies.

Berry, Santamarina, et al. [9] looked at the formation of vortices and stagnation regions between stent struts using a 2-D model of flow over a flat rigid plate. They found that large stagnation and separation regions could form between the struts for part or all of each cardiac cycle, and this behavior was dependent on stent size and spacing. Their observations agreed well with dye flow measurements they performed on a similar experimental setup.

The effect of coronary stent implantation on wall shear stresses (WSS) was examined by LaDisa et al. [23] in a three-dimensional CFD model of a slotted-tube stent in a rigid artery. Blood flow was imposed as steady parabolic profiles, neglecting the pulsatile variation. They also observed stagnation zones next to stent struts, and noted a decrease in minimum shear stress of up to 77% as compared to unstented arteries. The lowest values were localized near strut junctions and downstream of the stent outlet.

Fewer studies have looked at combining the effects of both the fluid mechanics and the elastic behavior of the vessel walls. Without the addition of the compliance of the vessel walls, the propagation of pressure waves through the arterial system is completely absent, and the effect of any pressure reflections from regions of increased stiffness, such as a stent or plaque, is missed. While there is a wealth of sources detailing computational and experimental efforts concerning pressure wave reflections in bifurcating vessels and arterial trees, there has not been a similar degree of investigation into reflections from areas of increased stiffness.

Tortoriello and Pedrizzetti [24] examined the effects of stent implantation on WSS using an axisymmetric 2-D numerical fluids-solids model, relying on a 1st order perturbative method to handle the walls, rather solving the full solids problem. Their analysis of pulsatile flows revealed that the compliance mismatch and overexpansion caused by the stent both enhanced the flow disruption in the stented region, reducing the minimum WSS and causing rapid variations in flow near the stent ends.

Alderson and Zamir [25] used analytical techniques to derive expressions for the magnitude of a sinusoidal pressure waveform in a compliant vessel with discrete segments of variable stiffness. They noted that reflections raised the pressure amplitude upstream of the rigid section, and that increased stiffness and segment length amplified this effect. However, this model considered only reflection, and not fluid velocities or wall deflections, and did not allow for arbitrary axial distributions of elastic modulus, radius, or thickness. Results were also limited to sinusoidal driving pressures, though more complex waveforms might be constructed using a Fourier-type wave summation.

Formaggia et al. [26] also investigated a one dimensional numerical model of a flexible artery with variable stiffness. Although mostly concerned with the development of the numerical techniques themselves, they did present some qualitative examinations of the effect of stent stiffness and length on the pressure within the vessel, and found that stiffer stents created larger upstream reflections, as did lengthening the prosthesis. However, their tests did not use physiologically correct values for the dimensions and physical properties of the system. In addition, their model was less able to deal with sudden discontinuities in the wall stiffness, and they did not examine the effect of variations of wall geometry. Nevertheless, the concepts outlined in their work provided a valuable guide in the effort presented here.

It was the goal of this research to develop an analytical tool to address some of these limitations by considering the interaction between the fluid mechanics of the blood and the solid mechanics of the vessel walls. The model developed here includes the coupling between the elastic motion of the walls and the flow in the stented artery, and allows for the specification of arbitrary vessel properties (wall thickness, radius, stiffness) along its length as well as the introduction of arbitrary pressure waveforms at the inlet. This model was then used to evaluate possible improvements in stent design. As the main measure of comparison was to be pressure wave reflection, consideration of the full three-dimensional flow was unnecessary and great gains in computational efficiency were achieved by focusing the analysis to a one-dimensional solution.

Methods

Governing Equations

The problem of wave propagation in a compliant artery can be modeled by an equation for continuity, and one for momentum. Since pressure wave transmission and reflection are inherently inviscid phenomena, the effects of the fluid viscosity can safely be omitted from the momentum equation. As a result these two equations form a system of the form

$$\frac{\partial q}{\partial t} + \frac{\partial F}{\partial x} = 0 \tag{1}$$

with

$$q = \begin{Bmatrix} A \\ u \end{Bmatrix} \text{ and } F = \begin{Bmatrix} uA \\ \frac{1}{2}u^2 + \frac{P}{\rho} \end{Bmatrix}, \tag{2}$$

which has three independent variables in x and t: area (A), pressure (P), and velocity (u). Here t and x are time and position, while fluid density, ρ, is taken to be constant equal to the normal density of human blood, (1057 kg/m^3).

To complete the solution, a third relationship is required. For this problem, an equation relating the applied internal pressure in the vessel to the wall deflection was derived based on Timoshenko and Woinowski-Krieger's work on cylindrical shells [27].

$$\frac{d^2}{dx^2}\left(D\frac{d^2 w}{dx^2} \right) + \frac{Eh}{r^2} w = P, \tag{3}$$

where D is defined as

$$D = \frac{Eh^3}{12\left(1-\nu^2\right)} \tag{4}$$

Here, r is the inner radius of the vessel (which can be rewritten in terms of A), the wall thickness is given by h, and w represents the deflection of the wall from neutral. The mechanical properties of the vessel wall are given by E, the elastic modulus, and ν, the Poisson's ratio. Both are functions of position, x, but are constant with time.

Using Equation (3), an examination of the contribution of the fourth order bending term to the overall deflection curves was conducted. For this comparison, the full solution to the equation was compared to results obtained by considering only the linear response of the vessel walls. Figure 1 shows the results of one such test for the Cordis CS30-035 stent design that will be used as a reference case below. Qualitatively it appears that the results are reasonably close,

and cause only a localized disturbance in the shape of the transition region between the stent border and the unstented vessel. While the magnitude of the relative errors, as referenced to the maximum deflection for the vessel (see Figure 2), appear large locally, it was decided this was an acceptable compromise, and that the first-order hoop term was the dominant effect in the conditions being examined. Equation (3) can then be written as a linear relationship between the applied internal pressure, and the square root of the vessel area:

$$P(x) = \beta(x)\left(\sqrt{A(x)} - \sqrt{A_0(x)}\right) + P_0\,, \tag{5}$$

where $\beta = \dfrac{4Eh}{3r_0^{\,2}\sqrt{\pi}}$ if the vessel wall is assumed to be incompressible. The suitability of this approximation is furthered reinforced by a consideration of the derivatives in Equations (1) and (2), since the pressure and area terms are present only as first-order derivatives in x.

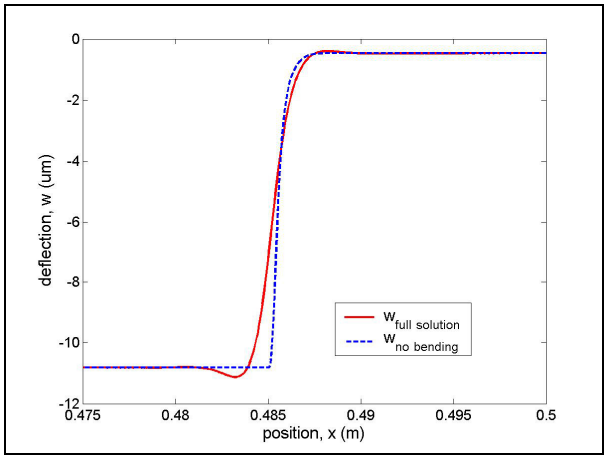

Figure 1: The bending terms smoothed the deflection profile near the stent, but had little overall affect on the shape of the curve.

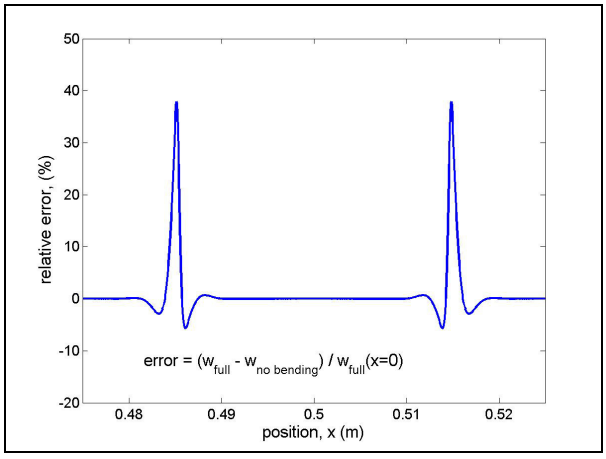

Figure 2: Errors from the no-bending approximation are localized to the stent ends, and are close to zero elsewhere.

Solution Method

In order to solve Equation (1) numerically, a weighted essentially non-oscillatory (WENO) scheme [28, 29] of order 3 was chosen for the spatial discretization. The details of the method used are described in [28] and [29]. These schemes have several advantages when solving problems with a mix of smooth regions and discontinuities. With the sudden changes in wall stiffness introduced by the stent, surrounded by large regions of little or no changes in properties, this problem is exemplary of these conditions. In this case, the third-order method used can maintain up to fifth-order accuracy throughout the region of interest without introducing spurious oscillations in the solution.

Time discretization was performed using a fourth-order, five-stage Runge-Kutta method. as described in [30] and [31]. This form was chosen to help minimize the memory requirements of the algorithm.

Boundary Conditions

Because the 3rd order WENO method requires the existence of 2 nodes left and right of each calculated node, it was necessary to generate extra points beyond the region of interest at each end of the domain. This was handled by reusing the current value of the first or last node in the domain, as appropriate, until there were sufficient nodes to perform the calculations near the boundaries.

In order to drive the flow through the vessel, it was assumed that the behavior of the system was governed by the entry of a pressure wave at the proximal entrance, to which the vessel area and velocity would respond. To simulate this, the pressure at either end was calculated as a function of time for each trial. This forcing function was then translated into an equivalent induced fluid velocity and the associated wall deflection was calculated by Equation (5). During the calculation of the solution, boundary conditions based on the method of characteristics were imposed upon the two end points.

Mesh Generation

For this study, the region of greatest interest is localized to the area surrounding the location of the stents (and the associated sharp gradient in wall compliance), while most of the remaining problem domain is smooth, containing no sudden changes in vessel properties. Initial trials indicated that generation of pressure wave reflection and other flow structures was limited to the area near regions of changing compliance, as was most of the interaction of intersecting pressure waves. To take advantage of this fact, the solver was modified to incorporate a variably spaced grid. Figure 3 shows the grid chosen for this study.

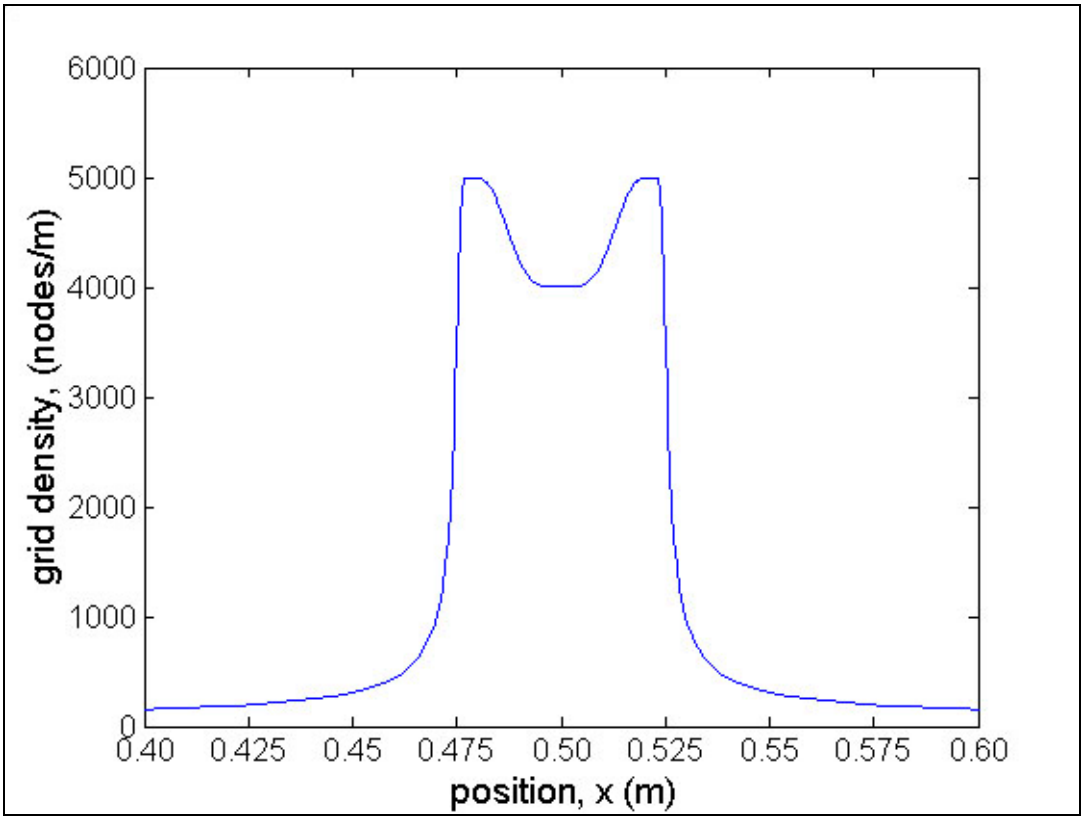

Figure 3: Variation in grid density near the stented region

The size of the time step used was calculated dynamically for each simulation based on the material properties of the vessel and grid spacing used in that trial. For stability, a maximum Courant number (CFL) of 1.0 was chosen. For each node in the problem domain the value for Δt required to yield the desired CFL was calculated, and from this set a Δt that would maintain a CFL less than or equal to 1.0 throughout the domain was chosen. Smaller values for Δx and stiffer vessels walls both required smaller Δt's. Because the regions of maximum stiffness and minimum grid spacing typically intersected, this led to very small values for Δt being required; typically Δt fell between $1x10^{-5}$ and $1x10^{-6}$.

Repeated testing of the solution at varying grid densities showed that for sufficiently fine grids, the solution was largely independent of grid selection. It was important, however, to maintain finer resolution around the stent ends, or the compliance transition would introduce time-independent local oscillations in the solution at these points.

Cases of Interest

The conditions chosen for the setup of the numerical model were based upon average values for left coronary arteries in humans aged 40 to 59 years [32]. Table 1 lists these base values. The pulse pressure, ΔP was based upon a systolic pressure of 120 mmHg and a diastolic pressure of 80 mmHg. Because the numerical model responds to changes in pressure, but the absolute pressure is unimportant, the lower bound for pressure was set at 0 mmHg for computational simplicity. The shape of the input pressure wave was chosen to be a series of half sine wave pulses with a constant resting pressure between each pulse. Figure 4 shows a plot of the waveform that was used as an input to the system at the vessel inlet.

The presence of the stent was handled by assuming the stent and the vessel walls together acted as a single, composite material. The effective stiffness of the stent-vessel system was calculated by numerical simulation of its mechanical properties in a commercial FEM package. The stent modeled was a standard Palmaz-type stent, similar to Cordis's CROWN stent. The results showed the effective modulus was approximately 50 MPa.

For the numerical model the stiffness along the length of the vessel was assumed to be a smoothly varying function, E(x). Figure 5 shows a schematic of E(x) for one of the cases tested. The baseline value corresponding to the vessel stiffness, E_0=2.19 MPa, was the same for all tests. The maximum stiffness of the stent-vessel system, E_1, depended on the exact case tested. In order to help understand how the stent scaling parameters interact, the stiffness ratio, E_1/E_0, for each trial will be compared instead of the actual value of E_1. Because of the way the stent edges interacted with the vessel walls, the compliance was assumed to transition gradually from E_0 to E_1, and the transition length, δ, was varied depending on the test case. This mimicked the way real stents can have struts of differing number and design at the two ends. To help compare stents with the same total stent length, but different transition lengths, a quantity called the effective stent length was defined to be the distance between the midpoints of the two transition regions.

Table 1: Base vessel and circulatory properties used for the simulation

Parameter	Value
Pulse pressure, ΔP	40 mmHg
Pulse frequency, f	1.33 Hz (80 bpm)
Fluid density, ρ	1057 kg/m^3
Base expanded radius, r_0	1.75 mm
Vessel wall thickness, h	0.69 mm
Vessel modulus of elasticity, E_0	2.19x10^6 Pa

The Cordis CS30-035 CROWN stent was chosen to serve as reference point for the geometric properties of the system [33]. This stent is 30 mm long when fully expanded, and has an inner radius of 1.75 mm. The vessel wall thickness, as mentioned above, remained 0.69 mm. A value of 3.0 mm was found to be a good estimate for the compliance transition zone length. The bold values in Table 2 correspond to these reference conditions. Based upon these values, several other values were chosen for each of these five parameters in order to create a reasonable range of conditions for testing.

Table 2: Vessel properties used for testing. The values for the Cordis CS30-035 stent, which were used as a reference for each characteristic, are shown in bold.

Characteristic	Tested Values
Stiffness ratio, E_1/E_0	2x, 5x, **22.9x**, 100x, 1000x
Total stent length, L (mm)	15, 22, **30**, 37, 45
Compliance transition zone length, δ (mm)	1, 2, **3**, 4, 5, 6
Vessel radius, r_0 (mm)	1.0, **1.75**, 3.0, 4.0, 5.0
Wall thickness, h (mm)	0.25, 0.5, **0.69**, 1.0

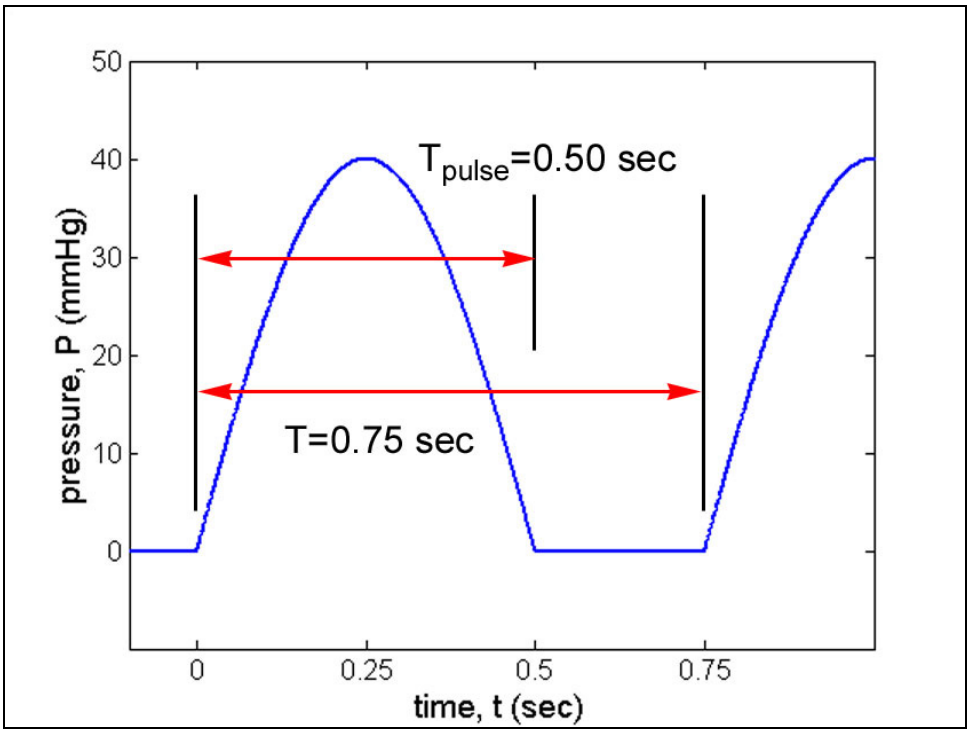

Figure 4: Pressure wave that was used as the input to the system.

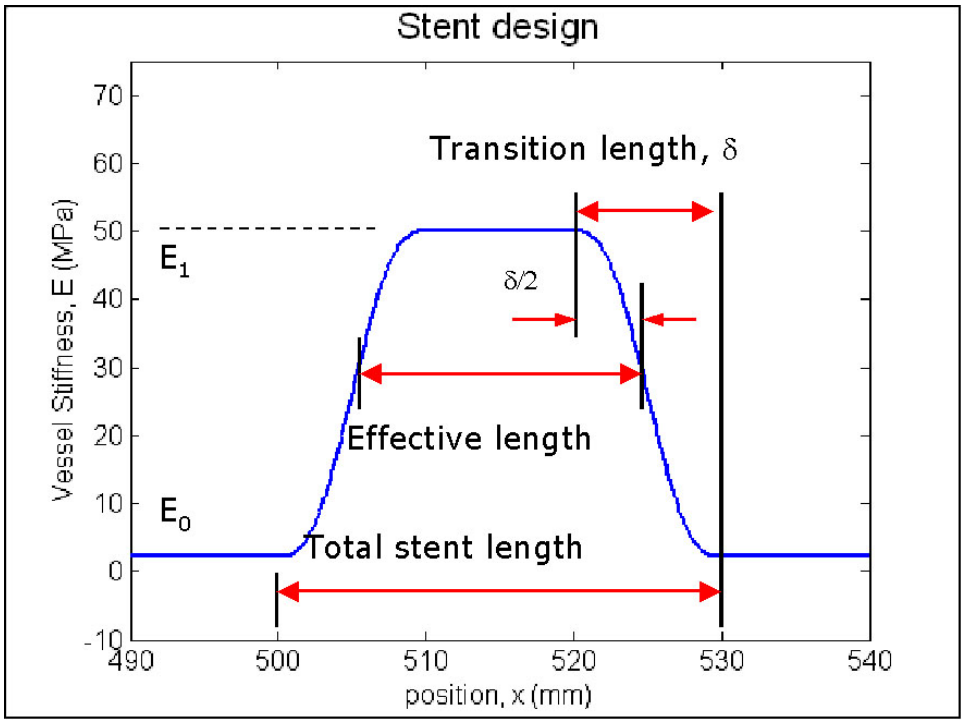

Figure 5: Diagram shows how the various test parameters, such as total stent length and transition length, influence the variation in stiffness along the length of the stent

Results

Figure 6 provides a summary of the relative magnitudes of the pressure reflections for some of the cases examined using the methods described above. In the trials shown here several groups were constructed by selecting a single parameter from Table 2 to change while the rest were held constant, allowing the relative effect of each change to be evaluated. It was found that varying several of the parameters examined could cause the magnitude of the pressure wave reflected from the stented region to vary more than 50% from the reference calculated for a Cordis CS30-35 CROWN stent, while changing the transition length had a relatively small effect on the reflections. For all cases tested, the reflected pressure wave demonstrated a sudden increase in pressure to the maximum magnitude, followed by a region during which the pressure slowly decreased towards an equal minimum value, and then a sudden correction back to zero. Figure 7 shows a plot of the pressure reflection recorded over time as the wave passes by a fixed point upstream of the stent. A comparison of this waveform shows it to be the same length and shape as the incident pressure waveform, but shifted 90 degrees out of phase.

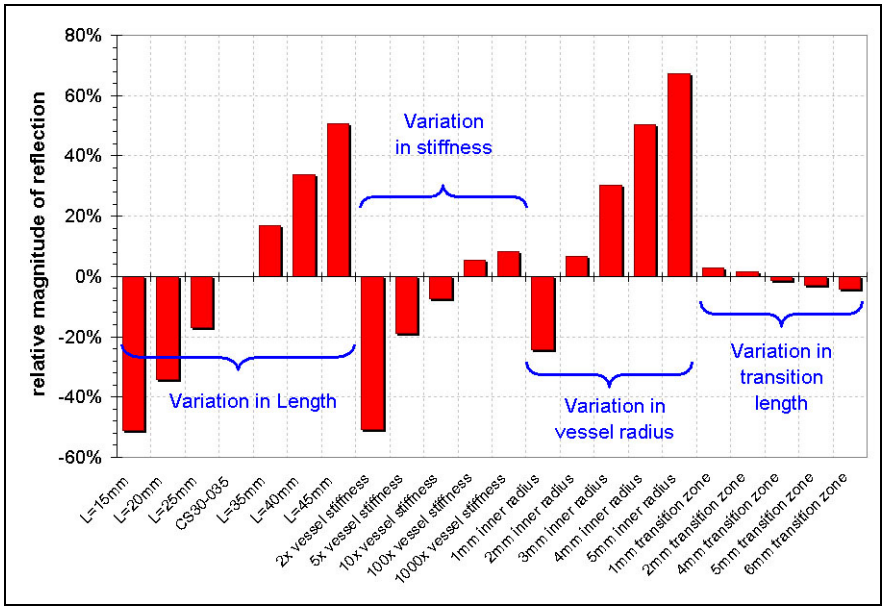

Figure 6: Relative change in the magnitude of the reflected pressure wave as compared to a Cordis CS30-035 CROWN Stent. Each test parameter was varied independently to observe their effect on the reflected pressure waves.

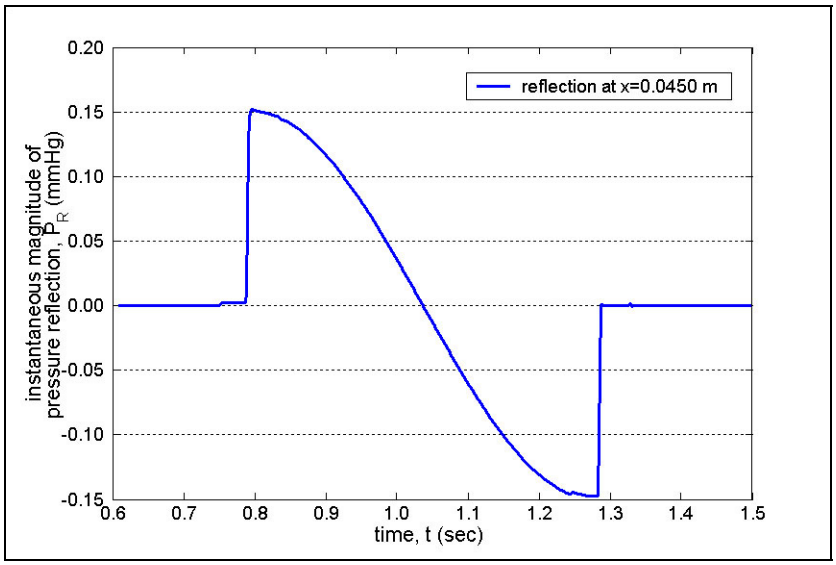

Figure 7: Plot of the shape of the reflected pressure wave for the reference case, which was typical of all tests. For each case the shape was similar, and only the magnitude of the pressure variation changed.

In a quantitative sense, the magnitude of the reflected pressure wave was found to vary linearly with length of the stent being tested. Figure 8 shows this relationship for several different values of the maximum vessel stiffness. As the stiffness of the vessel rose, the system became more sensitive to the length of the stent, and consequently the reflection increased more quickly with increasing length.

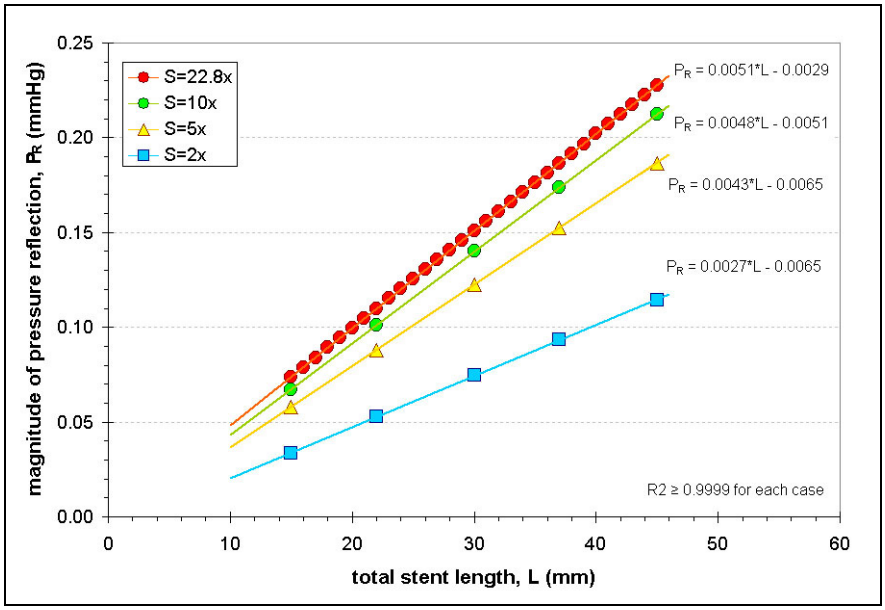

Figure 8: The magnitude of the reflected pressure wave increased linearly with total stent length if maximum stiffness was held constant.

Similarly, when the total length of the stent was held constant, but the length of the transition region was increased, the pressure reflection decreased in magnitude (Figure 9). These two parameters, stent length and transition length, can be lumped into a measurement of effective stent length. If this done, it can be seen that a linear relationship gives a good approximation of the reflection, but does not capture the entire behavior of the system. Figure 10 illustrates these results for a stent of maximum stiffness of 50 MPa ($E_1/E_0 = 22.8$).

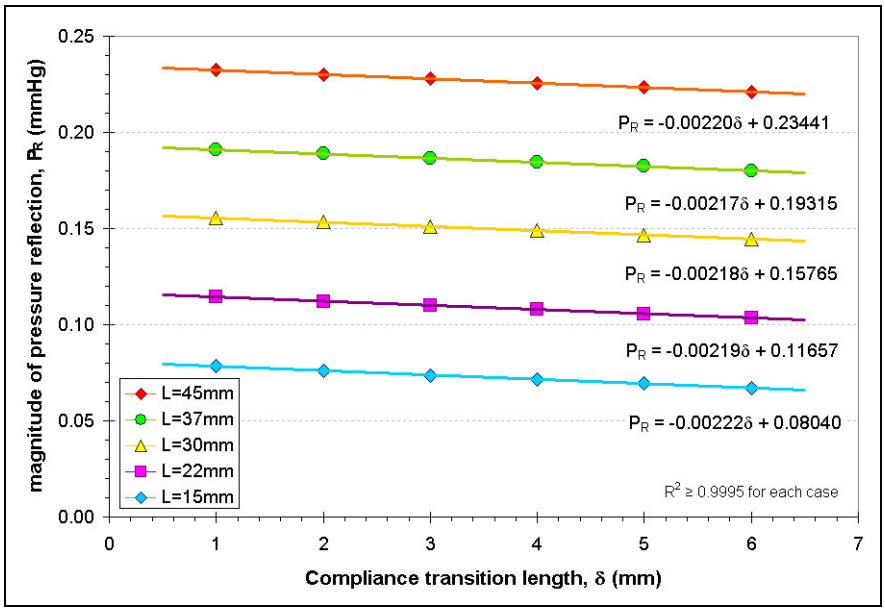

Figure 9: Pressure wave reflection decreased linearly with increasing transition length for a stent of constant total length.

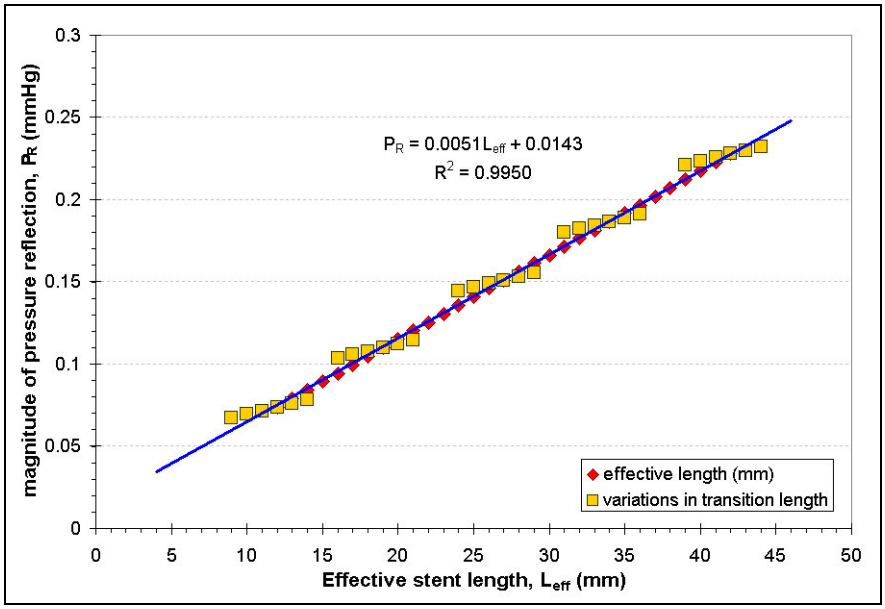

Figure 10: There is a correspondence between the reflection and the effective length of the stent, but the relationship is only approximately linear.

Next, the effect of the geometry of the vessel walls was examined by varying the inner radius and the wall thickness. As can be seen in Figure 11, for a constant stent and wall stiffness the magnitude of the reflected pressure wave increased approximately proportional to the square root of the vessel radius. Similarly, Figure 12 shows how the reflection decreased with the inverse of the square root of the wall thickness. Taken together, these two relationships suggested using a single non-dimensional parameter, $(R/h)^{1/2}$, to describe the effect of the vessel geometry on the magnitude of the pressure waves reflected from an implanted stent. Figure 13 shows how the calculation of this non-dimensional geometric parameter causes the results plotted in Figure 11 and Figure 12 to collapse onto a single line.

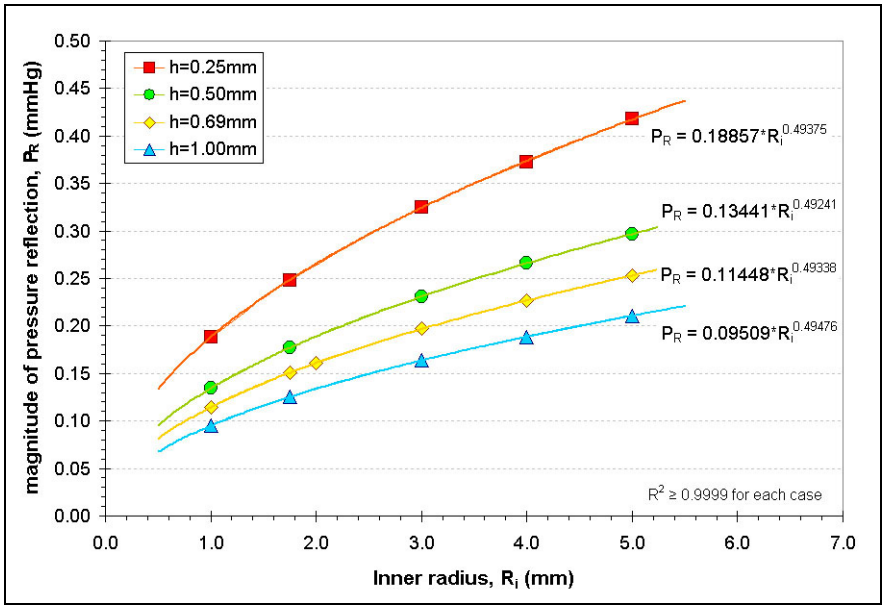

Figure 11: The pressure reflection increased with increasing vessel radius. This relationship appeared to be linear in the square root of the radius.

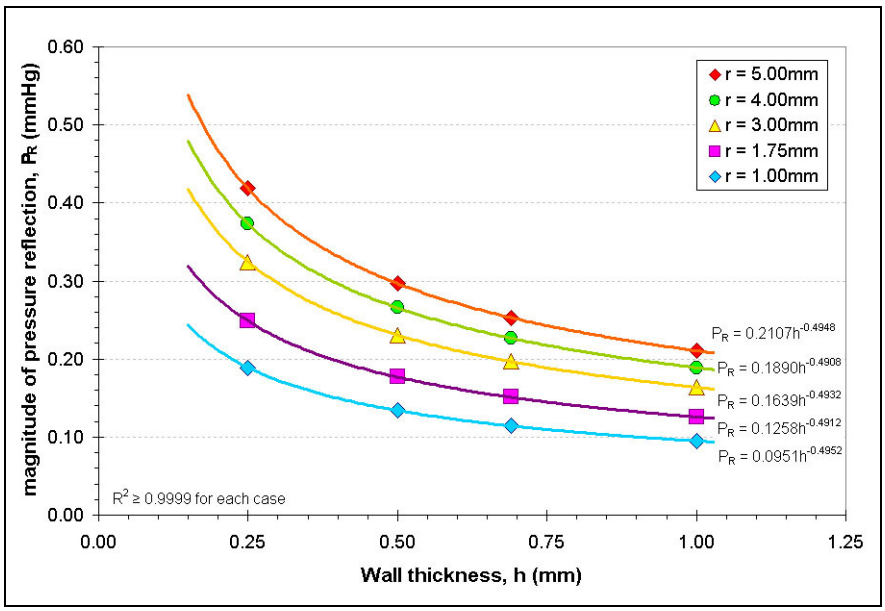

Figure 12: The magnitude of the reflected pressure wave decreased geometrically with increasing wall thickness. Once again, the geometry appears to be related to the reflection by the exponent of 0.5.

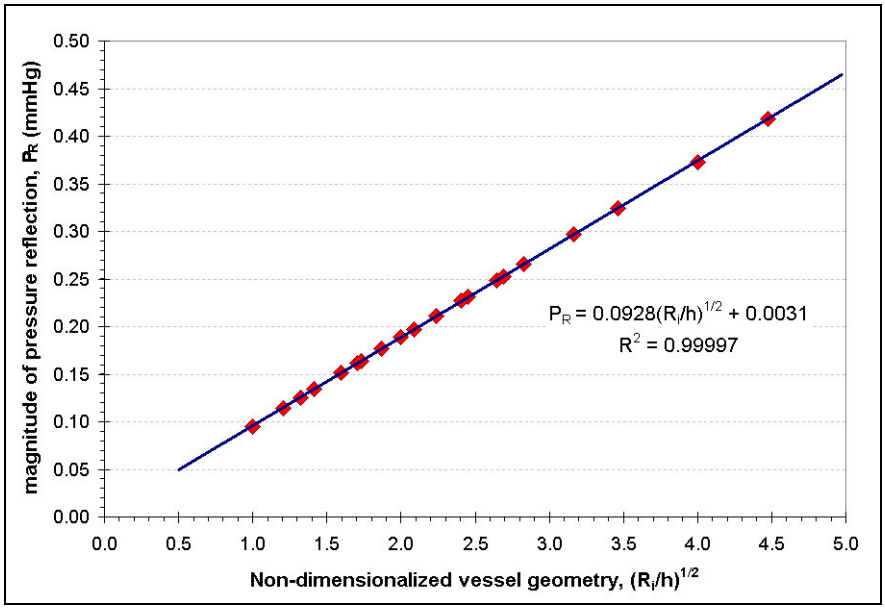

Figure 13: Combining the inner vessel radius with the wall thickness into a single non-dimensional parameter yielded a linear relationship between the reflection and the geometry of the vessel.

The effect of the stiffness of the stent relative to the vessel was also examined for several stent lengths between 15 to 45 mm. Figure 14 shows the pressure reflections calculated for each of these tests. From inspection of this plot, the relationship appears to be similar to a hyperbolic tangent, with the reflection assumed to be zero for a vessel in which any "stent" had the same compliance as the surrounding tissue, and asymptotically reaching a maximum value as the stiffness increased towards infinite.

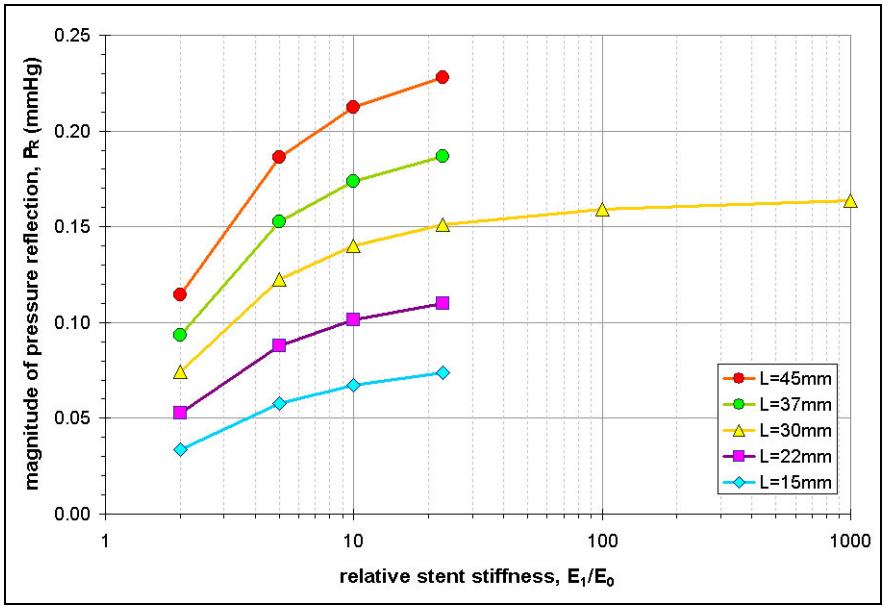

Figure 14: The relationship between the pressure reflection versus the stiffness ratio appears to be asymptotic. When plotted on a logarithmic scale, the curve closely resembles the plot of the hyperbolic tangent.

This suggested the development of a new non-dimensional parameter, here referred to as "stent authority," which might obey a relationship of the form

$$SA(x) = \tanh\left[\log\left(b\left(\frac{E_1}{E_0} - 1\right) + 1\right)\right]. \tag{6}$$

The stent authority can be calculated at every point in the vessel, and has a value between 0 (no stent or other arterial hardening present) and 1 (infinite stiffness). For the cases examined here the constant b was calculated to be approximately 2.198.

As can be seen in Figure 15, applying this equation resulted in a series of linear relationships between the peak stent authority (E_1 is defined as the maximum stiffness for each stent) and the magnitude of the reflected pressure wave. It is apparent that the length of the stented region also plays a role in determining the wave reflection and so, to account for variations in stiffness along the length of the vessel, the "Total Stent Authority" was also calculated by a simple integral,

$$total\ SA = \int_L SA(x)dx\,, \tag{7}$$

which has the effect of collapsing all the points in Figure 15 onto a single line. This concept of total stent authority also corrects the difficulties encountered in Figure 10 above. Figure 16 depicts the linear relationship between the pressure wave reflection and the total stent authority for each case. The plot includes tests examining variations in stent length, stiffness, and transition zone length.

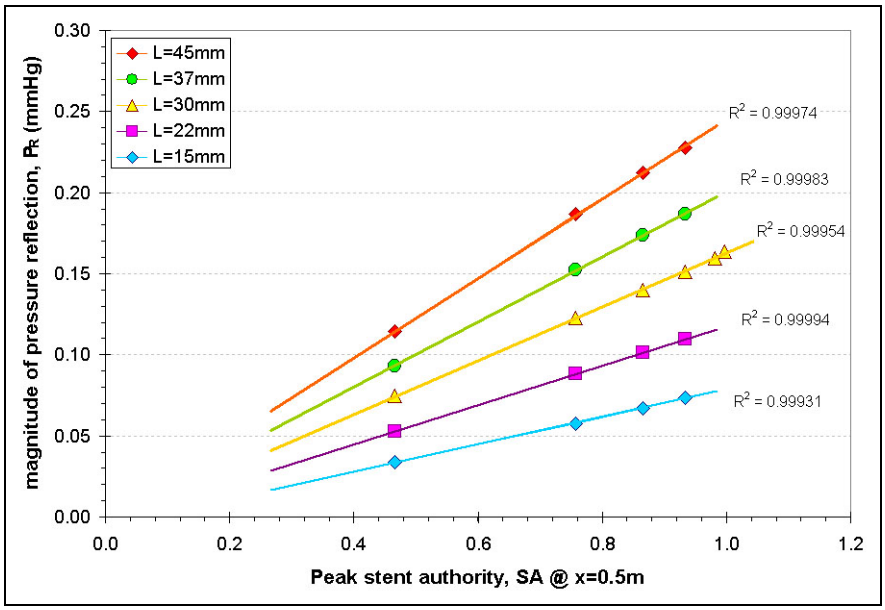

Figure 15: For a given stent length, the magnitude of the pressure reflection was observed to increase linearly with the stent authority as measured in the center of the stent. The reflection was more dependent on the stent stiffness when stent length was greater.

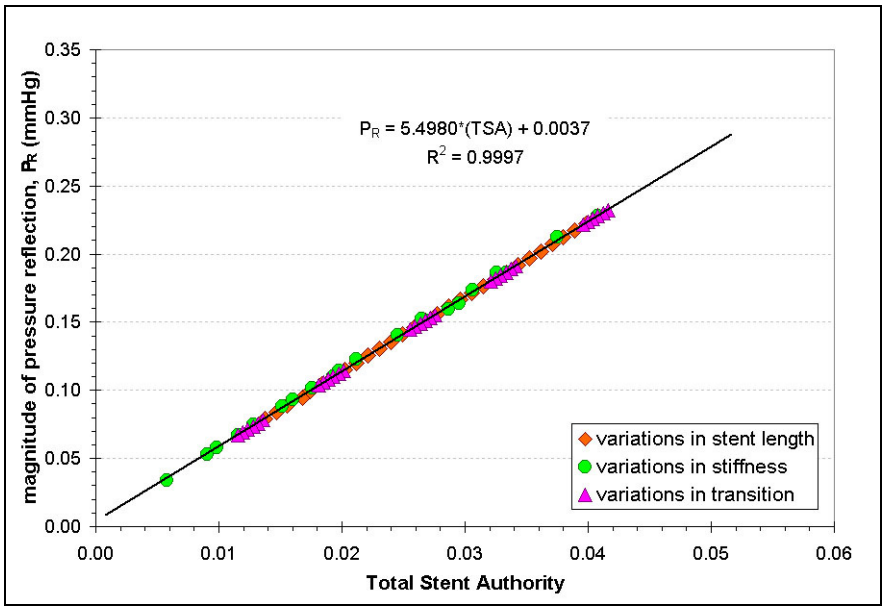

Figure 16: Total stent authority for each case corresponds very closely to the magnitude of the reflected pressure wave for that case.

The above formula neglects the effects of vessel geometry shown in Figure 11 and Figure 12, however. To account for variability in vessel radius and thickness of the vessel a term was added to the definition of stent authority, yielding an equation for "Geometric Stent Authority,"

$$GSA = \sqrt{\frac{r_0}{h}} \int_L \tanh\left[\log\left(b\left(\frac{E_1}{E_0} - 1\right) + 1\right)\right] dx \,. \tag{8}$$

It can be seen from Figure 17 that computing this parameter for each of the cases examined in this paper resulted in a simple linear relationship between the geometric stent authority and the resulting wave reflection.

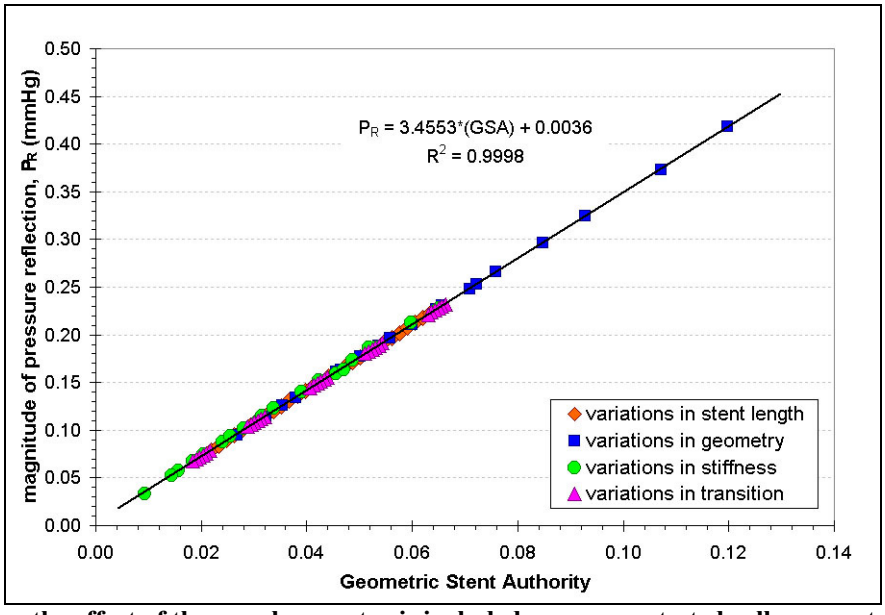

Figure 17: When the effect of the vessel geometry is included, every case tested collapses onto a single linear relationship between the reflection and the geometric stent authority.

Discussion

The results above demonstrate that variation in intravascular stent design can have a significant effect on the magnitude of the pressure waves reflected from the region of higher compliance created by that stent. Figure 6 showed that for the cases tested here this effect could be at least plus or minus 50% from the reference design. Thus, if a reduction in the pressure wave reflection caused by a stent is desired several factors should be considered in its design.

The first such consideration should be the total length of the stent chosen for implantation. It is clear from Figure 8 that the reflection is proportional to the stent length. As a result, the smallest stent that will provide adequate coverage of the vessel lesion should be chosen when planning an operation. This reinforces the results of several clinical studies that found a clear link between the length of the implanted stent and the likelihood that the patients would suffer from an adverse clinical outcome in the first few months [17,20].

Related to this is the stiffness of the stent itself. As would be expected, the model examined here predicts that the reflection drops off as the compliance of the stent approaches that of the vessel wall. This suggests that it would be wise to design stents to be as compliant as possible without compromising the intended function of the prosthesis. This is supported by clinical research [19], and many modern stents are less rigid than older designs.

Additionally, it has been shown that a gradual transition region can act to reduce the mechanical wall stresses imposed upon the artery, possibly improving the acute and chronic response of the vessel to the procedure [8]. One of the goals of this research was to determine if a similar reduction might be obtained for the wave reflection. However, these results show no benefit to a gradual compliance transition region at the ends of the stent, except as it reduces the effective length and total stent authority of the device. The magnitude of the reflection is unaffected by the transition zone length, and a design that remains rigid from end to end will not cause a negative effect.

The results of this model also suggest that the reflections will be greatest in vessels that have a larger radius and smaller wall thickness. It is not clear if there is a limit below which the reflected waves, already small, no longer have a physiological impact on the arterial system. Experimental research needs to be done to examine this issue.

Taken together, examination of the above effects led to the creation of a single a non-dimensional parameter referred to here as the "stent authority." This number appears to be a measure of how much of the incident pressure energy from the blood flow will be captured and reflected back upstream, relative to the energy the stent imposes upon the vessel. Assuming that experimental testing verifies this relationship, this is an extremely useful result, since it suggests that it is possible to quickly predict the magnitude of the pressure wave that will be reflected from a discontinuity in a vessel with compliant walls. For the conditions tested here, the resulting proportionality constant was approximately 3.46 mmHg per unit of Authority (GSA), but in general the precise relationship will depend on the magnitude of the incident pressure wave as well as the exact shape of the waveform in the time domain.

Another consideration is the relatively small magnitude of the reflected pressure waves compared to the magnitude of the fluctuations normally transmitted downstream in a healthy artery. Typical blood pressures can vary up to 40 mmHg per beat at a frequency of 1 to 2 Hz. The reflections predicted by this model for conditions matching these ranged from approximately 0.035 to 0.42 mmHg, or in other words at most only 1% of the total incident pressure variance is reflected proximally. Also, though not presented here, use of this model predicts similar reflection magnitudes for vessels containing reductions in lumen area. This suggests that

although the presence of irregularities, such as stenoses or coronary stents, along the length of a vessel does in fact lead to reflection of pressure waves back upstream, these reflections may not have much influence in-vivo for determining the subsequent health of an artery. If the presence of abnormal pressure reflections does lead to negative clinical outcomes, the role is probably not purely from the magnitude of the transmitted waves. Instead, it may have more to do with the introduction of sharp gradients in pressure within the vessel, as seen in Figure 7. An examination of the Navier-Stokes equations suggests that these pressure gradients may be related to the generation of vorticity and wall shear stress within the vessel, and can have an effect out of proportion to the associated magnitude of the pressure waves themselves. If this relationship proves valid, the geometric stent authority might then become a useful predictor of not only the magnitude of pressure reflections, but also the vorticity and wall shear stresses induced by the presence of a stent in an artery.

Conclusions

A one-dimensional numerical model for the reflection of pressure waves within a compliant, stented artery was created. The method chosen for this solution was a combination of an optimally 5^{th} order WENO method for spatial derivatives and a 4^{th} order Runge-Kutta method for time derivatives. This model was used to develop several relationships governing the magnitude of the pressure pulse reflected upstream off an implanted stent. It was found that an increase in relative stent stiffness, overall stent length, or lumen radius, or a decrease in arterial wall thickness, could lead to an increase in the magnitude of the wave reflection. These results suggest that to reduce wave reflections physicians should consider using only the smallest stent length that will successfully treat their patient. Additionally, because it was shown that more compliant stents create less wave reflection, designers of new prosthesis should favor designs that offer less rigidity. It was also shown that effect of the stent was proportionally greater in larger vessels. However, in contrast to analysis of mechanical wall stresses, it was not found that allowing a more gradual transition region between the vessel wall and the full stiffness of the stent had any impact on the magnitude of the wave reflection once the effect of the reduction in effective stent length was included in the analysis.

The total effect of all these properties was summarized in a single parameter referred to here as the "geometric stent authority." This number took the form shown in Equation (8), and appears to relate the energy imposed upon the vessel by the stent to the energy of the reflected pressure wave. If confirmed experimentally, this parameter could offer a simple way to evaluate the magnitude of the pressure wave that will be reflected from a new stent design without needing to perform detailed CFD or other similar numerical simulations.

Work is now planned to experimentally verify the conclusions of this numerical model in-vitro. Also, an extension of this work to axially symmetric or fully 3-D flow, elimination of the inviscid flow assumption, and consideration of the non-linear constitutive behavior of both blood and the arterial walls could provide important insights into additional physical behavior as well as help confirm the conclusions of this study.

References

1. American Heart Association, 2004, "Heart Disease and Stroke Statistics – 2004 Update."
2. American Heart Association, 2004, "International Cardiovascular Disease Statistics."
3. Dotter, C.T., 1969, "Transluminally-Placed Coilspring Endarterial Tube Grafts: Long Term Patency In Canine Popliteal Artery." Invest. Radiol., **4**, pp.329-332.
4. Topol E.J. , 1998, "Coronary-Artery Stents-Gauging, Gorging and Gouging," N Engl J Med **339**, pp. 1702-1704.
5. Knight, C.J., Curzen, N.P., Groves, P.H., Patel, D.J., Goodall, A.H., Wright, C., Clarke, D., Oldershaw, P.J., Fox, K.M., 1999, "Stent Implantation Reduces Restenosis in Patients With Suboptimal Results Following Coronary Angioplasty," European Heart Journal, **20**(24), pp. 1783-1790.
6. Edelman, E.R., Rogers, C., 1998, "Pathobiological Responses to Stenting," American Journal of Cardiology, **81**(7A), pp.4E-6E.
7. Babapulle, M.N., Eisenberg, M.J., 2002, "Coated Stents for the Prevention of Restenosis: Part I," Circulation, **106**, pp. 2734-2740.
8. Berry, J.L., Manoach, E., Mekkaoui, C., Rolland, P.H., Moore, J.E., Rachev, A., 2002, "Hemodynamics and Wall Mechanics of a Compliance Matching Stent: In Vitro and In Vivo Analysis," J. Vasc. Interv. Radiol., **13**, pp. 97–105.
9. Berry, J.L., Santamarina, A., Moore, J.E., Roychowdhury, S., Routh, W.D., 2000, "Experimental and Computational Flow Evaluation of Coronary Stents." Annals of Biomedical Engineering, **28**(4), pp. 386-398.
10. Kinlay, S., Grewal, J., Manuelin, D., Fang, J.C., Selwyn, A.P., Bittle, J.A., Ganz, P., 2002, "Coronary Flow Velocity and Disturbed Flow Predict Adverse Clinical Outcome After Coronary Angioplasty," Arterioscler. Thromb. Vasc. Biol. **22**, 1334-1240.
11. Wentzel, J.J., Gijsen, F.J.H., Stergiopulos, N., Serruys, P.W., Slager, C.J., Krams, R., 2003, "Shear stress, vascular remodeling and neointimal formation," Journal of Biomechanics, **36**, pp. 681-688.
12. Benard, N., Coisne, D., Donal, E., Perrault, R., 2003 "Experimental study of laminar blood flow through an artery treated by a stent implantation: characterization of intra-stent wall shear stress," Journal of Biomechanics **36**, pp. 991-998.
13. Babapulle, M. N., Eisenberg, M. J., 2002, "Coated Stents for the Prevention of Restenosis: Part II," Circulation **106**(22), pp. 2800-2805.
14. O'Neill, W.W., Leon, M.B., 2003, "Drug-Eluting Stents: Costs Versus Clinical Benefit," Circulation **107**(24), pp. 3008-3011.

15. Orlic, D., Bonizzoni, E., Stankovic, G., Airoldi, F., Chieffo, A., Corbaja, N., Sangiorgi, G., Ferror, M., Briguori, C., Montorfano, M., Calino, M., Colombo, A., 2004, "Treatment of Multivessel Coronary Artery Disease With Sirolimus-Eluting Stent Implantation: Immediate and Mid-Term Results," Journal of the American College of Cardiology, **43**(7), pp. 1154-1160.

16. Rogers, C., Edelman, E.R., 1995, "Endovascular Stent Design Dictates Experimental Restensois and Thrombosis," Circulation **91(**12), pp. 2995-3001.

17. Hausleiter, J., Kastrati, A., Mehilli, J., Schühlen, H., Pache, J., Dotzer, F., Dirschinger, J., Schömig, A., 2002 "Predictive Factors for Early Cardiac Events and Angiographic Restenosis After Coronary Stent Placement in Small Coronary Arteries," Journal of the American College of Cardiology, **40**(5), pp. 882-889.

18. Kastrati, A., Mehilli, J., Dirschinger, J., Dotzer, F., Schühlen, H., Neumann, F.-J., Fleckenstein, M., Pfafferott, C., Seyfarth, M., Schömig, A., 2001 "Intracoronary Stenting and Angiographic Results : Strut Thickness Effect on Restenosis Outcome (ISAR-STEREO) Trial," Circulation, **103**, pp. 2816-2821.

19. Pache, J., Kastrati, A., Mehilli, J., Schühlen, H., Dotzer, F., Hausleiter, J., Fleckenstein, M., Neumann, F.-J., Sattelberger, U., Schmitt, C., Müller, M., Dirschinger, J., Schömig, A., 2003, "Intracoronary Stenting and Angiographic Results: Strut Thickness Effect on Restenosis Outcome (ISAR-STEREO-2) Trial," Journal of the American College of Cardiology **41**(8), pp. 1283-1288.

20. Orlic, D., Bonizzoni, E., Stankovic, G., Airoldi, F., Chieffo, A., Corvaja, N., Sangiorgi, G., Ferraro, M., Briguori, C., Montofrano, M., Calino, M., Colombo, A., 2004, "Treatment of Multivessel Coronary Artery Disease With Sirolimus-Eluting Stent Implantation: Immediate and Mid-Term Results," Journal of the American College of Cardiology **43**(7) pp. 1154-1160.

21. Chua, S.N.D., MacDonald, B.J., Hashmi, M.S.J., 2002, "Finite-element simulation of stent expansion," Journal of Materials Processing Technology **120**, pp. 335-340.

22. Petrini, L., Migliavacca, F., Auricchio, F., Dubini, G., 2004, "Numerical investigation of the Intravascular coronary stent flexibility," Journal of Biomechanics **37**, pp. 495-501.

23. LaDisa, J.F. Jr., Guler, I., Olson, L.F., Hettrick, D.A., Kersten, J.R., Warltier, D.C., Pagel, P.S., 2003, "Three-Dimensional Computational Fluid Dynamics Modeling of Alterations in Coronary Wall Shear Stress Produced by Stent Implantation," Annals of Biomedical Engineering, **31,** pp. 972-980.

24. Tortoriello, A., Pedrizzetti, G., 2004, "Flow-tissue interaction with compliance mismatch in a model stented artery," Journal of Biomechanics **37,** pp. 1–11.

25. Alderson, H., Zamir, M., 2004, "Effects of stent stiffness on local haemodynamics with particular reference to wave reflections," Journal of Biomechanics **37**, pp. 339–348.

26. Formaggia, L., Nobile, F., and Quarteroni, A., 2001, "A one-dimensional model for blood flow: Application to vascular prosthesis," EPFL Report No. 02.2001, Dept. of Math, Lausanne, CH-1015, Switzerland.

27. Timoshenko, S., Woinowski-Krieger, S., 1959, *Theory of Plates and Shells, Second Edition*, McGraw-Hill Book Company, New York, Chap. 15.

28. Jiang, G.-S., Shu, C.-W., 1996, "Efficient Implementation of Weighted ENO Schemes," Journal of Computational Physics **126**, pp. 202-228.

29. Shu, C.-W., 2001, "High Order Finite Difference and Finite Volume WENO Schemes and Discontinuous Galerkin Methods for CFD," NASA CR-2001-210865 ICASE Report No. 2001-11.

30. Carpenter, M.H., Kennedy, L.A., 1994, "Fourth-Order, 2n-storage Runge-Kutta Schemes," NASA TM 109112, ICASE, NASA Langley Research Center.

31. Wilson, R.V., Demurren, A.O., Carpenter, M.H., 1998, "Higher-Order Compact Schemes for Numerical Simulation of Incompressible Flows," NASA CR-1998-206922 ICASE Report No 98-13.

32. Ozolanta, I., Tetere, G., Purinya, B., Kasyanov, V., 1998, "Changes in the Mechanical Properties, Biochemical Contents, and Wall Structure of the Human Coronary Arteries with Age and Sex," Medical Engineering & Physics **20**, pp. 523-533.

33. Cordis Corporation, 1998, "Information for Prescribers: PALMAZ-SCHATZ CROWN balloon-expandable Stent with PowerGrip Over-the-Wire delivery system," Cordis Corporation, a Johnson & Johnson company.

Appendix A: Simulation Code

The following code was originally written and compiled for FORTRAN. Additional details are available upon request.

```
      USE DFLIB

      IMPLICIT REAL*8(A-H,O-Z)
      parameter(nt=100001,nx=404,ntshort=10001)
      common /block1/ x(nx),t(nt)
      common /block2u/ u(nx,2)
      common /block2p/ p(nx,2)
      common /block2A/ A(nx,2)
      common /blk1/ area(-1:nx),uvel(-1:nx)
      common /block3/ pin(nt),uin(nt),ain(nt)
      common /block3a/ prr(nt),urr(nt),arr(nt)
      common /block4/ fa(nx),fu(nx)
      common /block5/ faj(nx,2),fuj(nx,2)
      common /block6/ ao(-1:nx),beta(-1:nx),YM(-1:nx)
      common /block6a/ r0(nx),c2(nx)
      common /block7/ cin(nt),crr(nt)
      common /block8t/ tsave(ntshort)
      common /block8p/ psave(nx,ntshort)
      common /block8u/ usave(nx,ntshort)
      common /block8a/ asave(nx,ntshort)
      common /gggg/ x_xi(nx),dxi
      common /dddd/ cro,rho
      common /pppp/ pmin
      common /ppp2/ pmax,tp
      common /nnnn/ npulse, n

      character*128 path
      integer(2) status
      integer(4) num
      logical(4) success

      namelist /param1/ x1,x2,xst1,xst2,delta,ro,ho,dr
c     namelist /param2/ cn,n,m
c     namelist /param2/ cn,dt,m,savestep
c     namelist /param2/ cn,dt,dtsave,m
      namelist /param2/ cn,dt,dtsave,time
      namelist /param3/ pmin,pmax,tp,npulse
      namelist /param4/ Eo,E1,rho

ccc   SET WORKING DIRECTORY
ccc   examine commandline for valid paths
ccc   try to change to that directory, quit if fail
ccc   default directory is ./

      if (NARGS( ).eq.2) then
       CALL getarg(1, path, status)
      else
       path   = '.'
       status = 1
      end if

      success = ChangeDirQQ(path)

c     write(*,*) success
c     write(*,*) path(1:status)

      if (success) then
       write(*,*) 'path='//path(1:status)
c      write(*,*) 'READING:'
c      write(*,*) path(1:status)//'/options.inp'
c      write(*,*) path(1:status)//'/grid.dat'
c      write(*,*) 'WRITING:'
c      write(*,*) path(1:status)//'/stiffness.inp'
      else
       num = GetLastErrorQQ()
       if (num.eq.ERR$NOMEM) then
        stop 'stopping: ERR$NOMEM'
       elseif (num.eq.ERR$NOENT) then
```

```
        write(*,*) path(1:status)//' is not a directory'
        stop 'stopping: ERR$NOENT'
       else
        stop 'stopping: unknown error'
       end if
      end if


ccc   OPEN files from working directory

      open(16,file='grid.dat')
      read(16,*) n
      read(16,*) ximin,ximax
      read(16,*) (x(j),j=1,n)
      read(16,*) (x_xi(j),j=1,n)
      dxi=(ximax-ximin)/dfloat(n-1)
      Hg=9.81d0*13.6d0

      open( 5,file='options.inp')
      open( 6,file='options.out')
      open( 7,file='properties.out')
      open( 8,file='scale.out')
      open( 9,file='stiffness.inp')
      open(10,file='radius.inp')
      read(5,param1)
      read(5,param2)
      read(5,param3)
      read(5,param4)

      if(n.gt.nx) then
       write(*,*) 'n>nx - insufficient allocation for space variables'
       stop
      end if

      pi=4.d0*datan(1.d0)
      pmin=pmin*Hg
      pmax=pmax*Hg

      read( 9,*) (YM(j),j=1,n)
      read(10,*) (r0(j),j=1,n)

      do 210 j=1,n
       YM(j)=YM(j)*Eo
210   continue

cccc  testing int division
c     write(*,*) 1,1
c     do 1234 j=2,100
c      write(*,*) j,(j-2)/10+2
c1234 continue
c     end test

cccc
cccc  Young's modulus as a function of x
c      Ay=10.d0
c      By=-15.d0
c      Cy=6.d0
c      do 212 j=1,n
c       YM(j)=Eo
c       if (x(j).gt.xst1.and.x(j).lt.xst2) then
c        YM(j)=E1
c        if (x(j).gt.xst1.and.x(j).lt.(xst1+delta)) then
c         eta=(x(j)-xst1)/delta
c         YM(j)=Eo+(E1-Eo)*(AY+By*eta+CY*eta**2)*eta**3
c        end if
c        if (x(j).lt.xst2.and.x(j).gt.(xst2-delta)) then
c         eta=(xst2-x(j))/delta
c         YM(j)=Eo+(E1-Eo)*(AY+By*eta+CY*eta**2)*eta**3
c        end if
c       end if
c 212  continue

c     write(6,777) (x(j),YM(j)/Eo,j=1,n)
 777  format(2E15.6)

cccc  Initial area distribution as a function of x
cccc   Assumptions: (1) If the pressure ( = pmax) is uniform (not a function of x)
cccc   the area, with radius = rmax (to be determined), is assumed to be calculated
cccc   by inflation of radius=r0(x) with no stent (YM(j)=YM(1))
ccc                 (2) If the pressure ( = pmin) is uniform (not a function of x)
cccc   the area is variable [ = ao(x)] to be determined such that its radius at x=0
```

```
cccc   is specified by ro. If YM~=constant, a0 may not equal pi*ro^2 everywhen
cccc
cccc   First, compute rmax:
      j=1
      dP=pmax-pmin
      c1=4.d0*ho*dsqrt(pi)/3.d0
c     ao(j)=pi*r0(j)**2
c     beta(j)=c1*YM(j)/ao(j)
c     rmax=r0(j)+dP/(dsqrt(pi)*beta(j))
c     c2=dsqrt(pi)*rmax


c     rx1=0.d0
      do j=1,n
cccc   First, compute rmax (assume YM[j]=YM[1]):
       ao(j)=pi*r0(j)**2
       beta(j)=c1*YM(1)/ao(j)
       rmax=r0(j)+dP/(dsqrt(pi)*beta(j))
       c2(j)=dsqrt(pi)*rmax

cccc   Second, compute ao(x) and then beta(x) exactly using quadratic formula:
       bracket=(c1*YM(j)/dP)*(c1*YM(j)/dP)+4.d0*c1*c2(j)*YM(j)/dP
       theta=1.d0/2.d0*(-c1*YM(j)/dP+dsqrt(bracket))
       ao(j)=theta*theta
       beta(j)=c1*YM(j)/ao(j)
c      rx=dsqrt(ao(j)/pi)
c      rx1=dmax1(rx,rx1)
      end do

c     write(*,*) rx1/ro


ccccccccccccccccccccccccccccccccccc
ccc   OLD METHOD (OBSOLETE):
cc   Second, compute beta(x) and ao(x), initially assume uniform ao(x), and then iterate
cc   to improve both beta and ao:
c     do j=1,n
c      ao(j)=pi*ro**2
c     end do
c
c     sqpi=dsqrt(pi)
c     c1=4.d0*ho*dsqrt(pi)/3.d0
ccc   iterate
c
c     do ki=1,10
c      do 214 j=1,n
c       beta(j)=c1*YM(j)/ao(j)
c214   continue
c      rx1=0.d0
c      do j=1,n
c       rx=rmax-(pmax-pmin)/(sqpi*beta(j))
c       ao(j)=pi*rx**2
c       rx1=dmax1(rx,rx1)
c      end do
c      write(*,*) ki,rx1/ro
c     end do
ccccccccccccccccccccccccccccccccccc

ccc   open(7,file='properties.out')
      write(7,603)
      write(7,604)
      write(7,605) (x(j),ao(j),YM(j),beta(j),j=1,n)
 603  format('       x[j] (m)    ao[j] (m^2)',
     &       '     YM[j] (Pa) beta[j] (Pa/m)')
 604  format('  -------------  -------------',
     &       '  -------------  -------------')
 605  format(4e15.6)

ccc   change this to a check
c     dt=1e9

ccc   open(8,file='scale.out')
      write(8,201)
      write(8,202)

ccccccccccccccccccccccccccccccccccccccccccccccccccc
ccc   calculate the timestep needed to fulfill stability

      write(*,*) 'requested dt=',dt

      do 216 j=1,n
```

```
       bbeta=beta(j)
       aao=ao(j)
       aaa=ao(j)
       call pofa(ppp,aaa,dpda,aao,bbeta,1)
       cro=dsqrt(aao*dpda/rho)
       dx=x_xi(j)*dxi
       dt1=cn*dx/cro
       write(8,203) x(j),cro,dt1
       dt=dmin1(dt1,dt)
 216  continue

      write(*,*) 'required dt=',dt

ccc   find the nskip needed to reduce dtsave to dt
      nskip = 1

      do 217 while (dtsave/nskip.gt.dt)
       nskip = nskip + 1
 217  enddo

      dt = dtsave/nskip

      write(*,*) 'dt=',dt
      write(*,*) 'dtsave=',dtsave
      write(*,*) 'nskip=',nskip

c     open(6,file='options.out')
      write(6,param1)
      write(6,param2)
      write(6,param3)
      write(6,param4)

      m = (time/dt)+1.0d0
c     write(*,*) 'm=',m
c     m = m+1
      write(*,*) 'm=',m
      write(*,*) 'final time=',(m-1)*dt
      write(6,*) 'm=',m

c      if(m.gt.nt) then
c      write(*,*) 'm>nt - insufficient allocation for time variables'
ccc    stop
c     end if



ccccccccccccccccccccccccccccccccccccccccccccccccc



 201  format('       x[j] (m)   cro[j] (m/s)',
     &       '    dt[j] (sec)')
 202  format('  -------------  -------------',
     &       '  -------------')
 203  format(3e15.6)


      write(6,204) dt
      write(*,204) dt
 204  format(' dt=',1e24.15e3)

ccccccccccccccccccccccccccccccccccccccccccccccc
ccc   setup time scale and BC's
ccccccccccccccccccccccccccccccccccccccccccccccc
      open(13,file='bc.out')
      write(13,607)
      write(13,608)
c602  format(i5,4e15.6)
 206   format(1e14.6e3)
 606  format(i15,4e15.6)
 607  format('      i (count)        t (sec)      uin (m/s)',
     &       '       pin (Pa)      ain (m^2)')
 608  format('  -------------  -------------  -------------',
     &       '  -------------  -------------')

c     itime   = 1
      moffset = 0

      if ( (nt).gt.(m) ) then
       call calcBCs(1,m,dt)
       write(13,606)(i,t(i),uin(i),pin(i)/hg,ain(i),
```

```
     &               i=1,m)
c      write(13,602)(i,t(i),urr(i),prr(i)/hg,arr(i),
c    &               i=1,m)
       else
        call calcBCs(1,nt,dt)
        write(13,606)(i,t(i),uin(i),pin(i)/hg,ain(i),
     &               i=1,nt)
c      write(13,602)(i,t(i),urr(i),prr(i),arr(i),
c    &               i=1,nt)
       end if



ccccccccccccccccccccc
c      initialize pressure, velocity, and area
       DO 30 j=1,n
        p(j,1)=pmin
        u(j,1)=0.d0
        ppp=p(j,1)
        aao=ao(j)
        bbeta=beta(j)
        call pofa(ppp,aaa,dpda,aao,bbeta,-1)
        a(j,1)=aaa
 30    CONTINUE
ccccccccccccccccccccc

       open(20,file='time.out')
       open(21,file='space.out')
       open(22,file='psave.out')
       open(23,file='asave.out')
       open(24,file='usave.out')

       itime=1

       tsave(itime) = t(itime)

       do j=1,n
        psave(j,itime)=p(j,1)/hg
        asave(j,itime)=a(j,1)/ao(1)
        usave(j,itime)=u(j,1)
       end do

c      write(22,206) ((psave(j,i), j=1,n), i=1 )
c      write(23,206) ((asave(j,i), j=1,n), i=1 )
c      write(24,206) ((usave(j,i), j=1,n), i=1 )

       noffset=0

       do 1000 itime=2,m
c      write(*,*) itime
ccccccccccccccccccccccccccccccc
       i=2
       do 50 j=1,n
        area(j) =a(j,i-1)
        uvel(j) =u(j,i-1)
 50    continue

       call weno (n,dt)

       do 106 j=2,n-1
        a(j,i)=area(j)
        u(j,i)=uvel(j)
 106   continue

ccccccccccc

       do 60 j=2,n-1
        aaa=a(j,i)
        aao=ao(j)
        bbeta=beta(j)
        call pofa(ppp,aaa,dpda,aao,bbeta,1)
        p(j,i)=ppp
 60    continue

cccccc Boundary condition at j=1
       frrw=4.d0*cin(itime-1-moffset*nt)+uin(itime-1-moffset*nt)
       ppp=p(1,i-1)
       aaa=a(1,i-1)
       aao=ao(1)
       bbeta=beta(1)
```

```
      call pofa(ppp,aaa,dpda,aao,bbeta,-1)
      cr1=dsqrt(aaa*dpda/rho)
      ppp=p(2,i-1)
      aaa=a(2,i-1)
      aao=ao(2)
      bbeta=beta(2)
      call pofa(ppp,aaa,dpda,aao,bbeta,-1)
      cr2=dsqrt(aaa*dpda/rho)
      glrw1=4.d0*cr1-u(1,i-1)
      glrw2=4.d0*cr2-u(2,i-1)
      dx=x_xi(1)*dxi
      cn1=(cr2-u(2,i-1))*dt/dx
      glrw=cn1*glrw2+(1.d0-cn1)*glrw1
      cr    =0.125d0*(frrw+glrw)
      u(1,i)=0.5d0*(frrw-glrw)
      a(1,i)=(2.d0*rho*cr**2/beta(1))**2
      bbeta=beta(1)
      aao=ao(1)
      aaa=a(1,i)
      call pofa(ppp,aaa,dpda,aao,bbeta,1)
      p(1,i)=ppp

cccccccc Boundary condition at j=n
      ppp=p(n,i-1)
      aaa=a(n,i-1)
      aao=ao(n)
      bbeta=beta(n)
      call pofa(ppp,aaa,dpda,aao,bbeta,-1)
      cr1=dsqrt(aaa*dpda/rho)
      ppp=p(n-1,i-1)
      aaa=a(n-1,i-1)
      aao=ao(n-1)
      bbeta=beta(n-1)
      call pofa(ppp,aaa,dpda,aao,bbeta,-1)
      cr2=dsqrt(aaa*dpda/rho)
      frrw2=4.d0*cr2+u(n-1,i-1)
      frrw1=4.d0*cr1+u(n  ,i-1)
      dx=x_xi(n)*dxi
      cn1=(cr2+u(n-1,i-1))*dt/dx
      frrw=cn1*frrw2+(1.d0-cn1)*frrw1
      glrw=4.d0*crr(itime-1-moffset*nt)-urr(itime-1-moffset*nt)
      cr    =0.125d0*(frrw+glrw)
      u(n,i)=0.5d0*(frrw-glrw)
      a(n,i)=(2.d0*rho*cr**2/beta(n))**2
      bbeta=beta(n)
      aao=ao(n)
      aaa=a(n,i)
      call pofa(ppp,aaa,dpda,aao,bbeta,1)
      p(n,i)=ppp
      do 770 j=1,n
      a(j,1)=a(j,2)
      u(j,1)=u(j,2)
      p(j,1)=p(j,2)
 770  continue

      if ( (itime-moffset*nt).gt.(nt) ) then
       moffset = moffset+1

       if ( (itime+nt-1).gt.(m) ) then
        call calcBCs(itime,m,dt)
c       write(20,206) ( t(i),
c     &             i=itime-nt*moffset,m-nt*moffset,nskip)
c       if (i-nskip.ne.m) then
c        write(20,206) ( t(m-nt*moffset) )
c       end if
        write(13,606)(i+nt*moffset,t(i),uin(i),pin(i)/hg,ain(i),
     &                i=itime-nt*moffset,m-nt*moffset)
c       write(13,602)(i+nt*offset,t(i),urr(i),prr(i)/hg,arr(i),
c    &                i=itime-nt*moffset,m-nt*moffset)
       else
        call calcBCs(itime,(itime+nt-1),dt)
        write(13,606)(i+nt*moffset,t(i),uin(i),pin(i)/hg,ain(i),
     &                i=itime-nt*moffset,(itime+nt-1)-nt*moffset)
c       write(13,602)(i+nt*offset,t(i),urr(i),prr(i),arr(i),
c    &                i=itime-nt*moffset,(itime+nt-1)-nt*moffset)
       end if
      end if


      if ( ((itime-2)/nskip+2).gt.((noffset+1)*ntshort) ) then
c      dump memory to disk to make more room
```

```
       write(20,206) ( tsave(i),           i=1,ntshort )
       write(22,206) ((psave(j,i), j=1,n), i=1,ntshort )
       write(23,206) ((asave(j,i), j=1,n), i=1,ntshort )
       write(24,206) ((usave(j,i), j=1,n), i=1,ntshort )
       noffset = noffset+1
      end if

c     assuming nskip=10, save routine
c     overwrites all but the 11th(2), 21st(3), ....
c     similarly for nskip=100, etc
c     itime=1 should already be saved
      do j=1,n
       tsave(  ((itime-2)/nskip+2-noffset*ntshort) )=t(itime-nt*moffset)
       psave(j, ((itime-2)/nskip+2-noffset*ntshort) )=p(j,1)/hg
       asave(j, ((itime-2)/nskip+2-noffset*ntshort) )=a(j,1)/ao(1)
       usave(j, ((itime-2)/nskip+2-noffset*ntshort) )=u(j,1)
      end do

c     write(*,*) itime,((itime-2)/nskip+2),t(itime)


 1000 continue




ccccccccccccccccccccccccccccccccccccccccccccccccccc
c         mplot=m/100
c         WRITE(33,204)
c         WRITE(33,205) n,mplot
c         WRITE(33,206) ((     x(i) , i=1,n), j=100,m,100)
c         WRITE(33,206) ((     t(j) , i=1,n), j=100,m,100)
c         WRITE(33,206) ((psave(i,j), i=1,n), j=100,m,100)
c
c204      FORMAT('variables=','"x"', ',', '"t"', ',',
c     &           '"p"')
c205      FORMAT('zone i=',I5,',', 'j=',I5, ',', 'F=BLOCK')
c206      FORMAT(4(E12.6, 2X))
c
c      write(88,801) (j,x(j),a(j,1)/ao(1),u(j,1),p(j,1)/hg,j=1,n)
c 801  format(i6,4e15.6)
c      write(9,601)(t(i),psave(1,i),psave(2,i),psave(3,i)
c     &                 ,psave(4,i),psave(5,i),i=1,m)
c     write(10,601)(t(i),usave(i,1),usave(i,2),usave(i,3)
c    &                 ,usave(i,4),usave(i,5),i=1,m)
c 601  format(6e13.5)
ccccccccccccccccccccccccccccccccccccccccccccccccccc

ccc   -> moved above main loop <-
c     open(20,file='time.out')
c     open(21,file='space.out')
c     open(22,file='psave.out')
c     open(23,file='asave.out')
c     open(24,file='usave.out')

c     i=1
c     do while (i.le.((m-2)/nskip+2) )
c      write(20,206) ( t(i) )
c      write(*,*) i, t(i)
c      i = i+nskip
c     end do

c     write(*,*) (i, i=1,((m-2)/nskip+2))

c     write(20,206) ( i, t(i), i=1,((m-2)/nskip+2))

c     write(20,206) ( t(i), i=1,m,nskip)
cc    write(*,*) i
c     if (i-nskip.ne.m) then
c      write(20,206) ( t(m) )
c     end if

      write(20,206) ( tsave(i), i=1, (m-2)/nskip+2-noffset*ntshort )
      write(21,206) ( x(j), j=1,n )
ccc   change these to include offsets on lower bound
c     ((itime-2)/nskip+2-noffset*ntshort)
      write(22,206) ((psave(j,i), j=1,n),
```

```
     &                i=1, (m-2)/nskip+2-noffset*ntshort )
      write(23,206) ((asave(j,i), j=1,n),
     &                i=1, (m-2)/nskip+2-noffset*ntshort )
      write(24,206) ((usave(j,i), j=1,n),
     &                i=1, (m-2)/nskip+2-noffset*ntshort )

c206   format(1e14.6e3)
207   format(i5,1e14.6e3)

      END


      subroutine pofa(p,a,dpda,ao,beta,ind)
      IMPLICIT REAL*8(A-H,O-Z)
      common /pppp/ pmin
      if(ind.eq.1) then
ccc   given a find p and partial dp/da
      p=beta*(dsqrt(a)-dsqrt(ao))+pmin
      dpda=0.5d0*beta/dsqrt(a)
      else
ccc   given p find a and partial dp/da
      a=(((p-pmin)/beta)+dsqrt(ao))**2
      dpda=0.5d0*beta/dsqrt(a)
      end if
      return
      end


      subroutine pofak9(p,a,dpda,ao,ind)
      IMPLICIT REAL*8(A-H,O-Z)
      itmax=100
      eps=0.1e-6
      pi=4.d0*datan(1.d0)
      sigma=1172.63d0
      beta=8.36483d0
      rmh=9.5d0
      if(ind.eq.1) then
ccc   given area, find pressure
      r=dsqrt(a/pi)
      ro=dsqrt(ao/pi)
      rr=r/ro
      expr=dexp(beta*(rr-1.d0))
      top=sigma*(expr-1.d0)
      bot=rmh*rr**2-0.5d0
      p=top/bot
      dadr=2.d0*pi*r
      dtop=sigma*beta*expr/ro
      dbot=2.d0*rmh*r/ro**2
      dpdr=(bot*dtop-top*dbot)/bot**2
      dpda=dpdr/dadr
      else
ccc   given pressure, find area
ccc   initial guess for r
      ro=dsqrt(ao/pi)
      rr=1.001
      do 10 it=1,itmax
      bot=rmh*rr**2-0.5d0
      rro=rr
      rr=1.d0+dlog(1.d0+(p/sigma)*bot)/beta
      if(dabs(rr-rro).lt.eps) go to 11
 10   continue
      write(6,*) it
 11   continue
      r=rr*ro
      a=pi*r**2
      expr=dexp(beta*(rr-1.d0))
      top=sigma*(expr-1.d0)
      bot=rmh*rr**2-0.5d0
      dadr=2.d0*pi*r
      dtop=sigma*beta*expr/ro
      dbot=2.d0*rmh*r/ro**2
      dpdr=(bot*dtop-top*dbot)/bot**2
      dpda=dpdr/dadr
      end if
      return
      end


      subroutine weno (imax1,dt1)
      implicit real*8(a-h,o-z)
      PARAMETER(nx=404,NSTAGE=5)
```

```
      COMMON /QQQQ/ Q1(-1:NX),Q2(-1:NX),Q3(-1:NX)
      COMMON /QQPP/ QP1(NX),QP2(NX),QP3(NX)
      common /gggg/ x_xi(nx),dxi
      COMMON /NIJK/ IMAX
      COMMON /STEP/ DX,DT,CFL
      common /blk1/ area(-1:nx),uvel(-1:nx)
      common /blk2/ rhs(nx,2)
      common /blk3/ ark(0:nstage),brk(nstage)
      imax=imax1
      dt=dt1
      ark(0)=0.d0
      ark(1)=-0.41789047d0
      ark(2)=-1.19215169d0
      ark(3)=-1.69778469d0
      ark(4)=-1.51418344d0
      brk(1)=0.14965902d0
      brk(2)=0.37921031d0
      brk(3)=0.82295502d0
      brk(4)=0.69945045d0
      brk(5)=0.15305724d0
      call weno_points
      DO 34 I=-1,IMAx+2
      Q1(I)  = area(i)
      Q2(I)  = uvel(i)
 34   CONTINUE
      CALL RK45
      DO 50 I=2,IMAx-1
      area(i)= Q1(I)
      uvel(i)= Q2(I)
 50   CONTINUE
      return
      end


      subroutine RK45
      implicit real*8(a-h,o-z)
      PARAMETER(nx=404,NSTAGE=5)
      COMMON /QQQQ/ Q1(-1:NX),Q2(-1:NX),Q3(-1:NX)
      COMMON /QQPP/ QP1(NX),QP2(NX),QP3(NX)
      common /gggg/ x_xi(nx),dxi
      COMMON /STEP/ DX,DT,CFL
      COMMON /NIJK/ IMAX
      common /blk2/ rhs(nx,2)
      common /blk3/ ark(0:nstage),brk(nstage)
      DO 150 KK=1,NSTAGE
      call res
      DO 140 I=2,IMAx-1
      qp1(i)=rhs(i,1)+ark(kk-1)*qp1(I)
      qp2(i)=rhs(i,2)+ark(kk-1)*qp2(I)
  140 CONTINUE
      DO 143 I=2,IMAx-1
      Q1(i)=q1(i)+dt*brk(kk)*qp1(I)
      Q2(i)=q2(i)+dt*brk(kk)*qp2(I)
  143 CONTINUE
  150 CONTINUE
      return
      END


      subroutine weno_points
      implicit real*8(a-h,o-z)
      PARAMETER(nx=404,mm=2)
      COMMON /NIJK/ IMAX
      common /block6/ ao(-1:nx),beta(-1:nx),YM(-1:nx)
      common /blk1/ area(-1:nx),uvel(-1:nx)
      do j=1,2
      ao(j-2)=ao(1)
      beta(j-2)=beta(1)
      area(j-2)=area(1)
      uvel(j-2)=uvel(1)
      ao(imax+j)=ao(imax)
      beta(imax+j)=beta(imax)
      area(imax+j)=area(imax)
      uvel(imax+j)=uvel(imax)
      end do
      return
      end


ccccccccccccccccccccccccccccccccc
cc    Compact scheme
```

```
ccccccccccccccccccccccccccccccccc
      subroutine res
      implicit real*8(a-h,o-z)
      PARAMETER(nx=404,mm=2)
      COMMON /QQQQ/ Q1(-1:NX),Q2(-1:NX),Q3(-1:NX)
      COMMON /STEP/ DX,DT,CFL
      COMMON /NIJK/ IMAX
      common /pppp/ pmin
      common /block6/ ao(-1:nx),beta(-1:nx),YM(-1:nx)
      common /gggg/ x_xi(nx),dxi
      common /dddd/ cro,rho
      common /blk2/ rhs(nx,2)
      common /work1/ split,press,Fnp,Fnm
      common /work2/ fp1,fp2,fp3,sp1,sp2,sp3
      common /work3/ fm1,fm2,fm3,sm1,sm2,sm3
      common /work4/ fL1,fL2,fL3
      common /work5/ fR1,fR2,fR3
      common /work6/ wfL,wfR
      common /work7/ fn
      dimension split(-1:nx),press(-1:nx)
      dimension Fnp(-2:2,-1:nx,mm),Fnm(-2:2,-1:nx,mm)
      dimension fp1(-1:nx,mm),fp2(-1:nx,mm),fp3(-1:nx,mm)
      dimension sp1(-1:nx,mm),sp2(-1:nx,mm),sp3(-1:nx,mm)
      dimension fm1(-1:nx,mm),fm2(-1:nx,mm),fm3(-1:nx,mm)
      dimension sm1(-1:nx,mm),sm2(-1:nx,mm),sm3(-1:nx,mm)
      dimension fL1(-1:nx,mm),fL2(-1:nx,mm),fL3(-1:nx,mm)
      dimension fR1(-1:nx,mm),fR2(-1:nx,mm),fR3(-1:nx,mm)
      dimension wfL(-1:nx,mm),wfR(-1:nx,mm)
      dimension fn(-1:nx,mm)
      eps=1.d-6
      do 112 i=-1,imax+1
      A      = 0.5d0*(q1(i)+q1(i+1))
      bbeta  = 0.5d0*(beta(i)+beta(i+1))
      aao    = 0.5d0*(ao(i)+ao(i+1))
      dpda   = 0.5d0*bbeta/dsqrt(A)
      C      = dsqrt(A*dpda/rho)
c     following line caused problems, orginally u=0
c     U      = 0.5d0*(q2(i)+q2(i+1))
      U      = 0
      split(i) = 1.0d0*(abs(u)+c)
 112  continue
      do 114 i=-1,imax+2
      A      = q1(i)
      bbeta  = beta(i)
      aao    = ao(i)
      p=bbeta*(dsqrt(A)-dsqrt(aao))+pmin
      press(i)= p
 114  continue
      do 120 i=1,imax-0
      do 120 j=-2,2
      A      = q1(i+j)
      U      = q2(i+j)
      bbeta  = beta(i+j)
      aao    = ao(i+j)
      p      = press(i+j)
      Fnp(j,i,1)  = U*A              +split(i)*A
      Fnp(j,i,2)  = 0.5d0*U*U+P/rho  +split(i)*U
      Fnm(j,i,1)  = U*A              -split(i-1)*A
      Fnm(j,i,2)  = 0.5d0*U*U+P/rho  -split(i-1)*U
 120  continue
ccc
      do 100 m=1,mm
      do 100 i=1,imax-0
      fp1(i,m)= 0.5d0*(fnp(-2,i,m)-4.d0*fnp(-1,i,m)+3.d0*fnp(0,i,m))
      fp2(i,m)= 0.5d0*(fnp( 1,i,m)-     fnp(-1,i,m)                 )
      fp3(i,m)=-0.5d0*(fnp( 2,i,m)-4.d0*fnp( 1,i,m)+3.d0*fnp(0,i,m))

      sp1(i,m)= fnp(-2,i,m)-2.d0*fnp(-1,i,m)+fnp( 0,i,m)
      sp2(i,m)= fnp( 1,i,m)-2.d0*fnp( 0,i,m)+fnp(-1,i,m)
      sp3(i,m)= fnp( 2,i,m)-2.d0*fnp( 1,i,m)+fnp( 0,i,m)

      fm1(i,m)= 0.5d0*(fnm(-2,i,m)-4.d0*fnm(-1,i,m)+3.d0*fnm(0,i,m))
      fm2(i,m)= 0.5d0*(fnm( 1,i,m)-     fnm(-1,i,m)                 )
      fm3(i,m)=-0.5d0*(fnm( 2,i,m)-4.d0*fnm( 1,i,m)+3.d0*fnm(0,i,m))

      sm1(i,m)= fnm(-2,i,m)-2.d0*fnm(-1,i,m)+fnm( 0,i,m)
      sm2(i,m)= fnm( 1,i,m)-2.d0*fnm( 0,i,m)+fnm(-1,i,m)
      sm3(i,m)= fnm( 2,i,m)-2.d0*fnm( 1,i,m)+fnm( 0,i,m)
 100  continue
      hh=0.5d0
      hh2=1.d0/8.d0
```

```
c     hh=0.0d0
c     hh2=0.d0/8.d0
      do 200 m=1,mm
      do 200 i=1,imax-0
      fL1(i,m)=fnp(0,i,m)+hh*fp1(i,m)+hh2*sp1(i,m)
      fL2(i,m)=fnp(0,i,m)+hh*fp2(i,m)+hh2*sp2(i,m)
      fL3(i,m)=fnp(0,i,m)+hh*fp3(i,m)+hh2*sp3(i,m)
      fR1(i,m)=fnm(0,i,m)-hh*fm1(i,m)+hh2*sm1(i,m)
      fR2(i,m)=fnm(0,i,m)-hh*fm2(i,m)+hh2*sm2(i,m)
      fR3(i,m)=fnm(0,i,m)-hh*fm3(i,m)+hh2*sm3(i,m)
 200  continue
      CL1=1.d0/16.d0
      CL2=10.d0/16.d0
      CL3=5.d0/16.d0
      CR1=5.d0/16.d0
      CR2=10.d0/16.d0
      CR3=1.d0/16.d0
      do 300 m=1,mm
      do 300 i=1,imax-0
      rL1=(eps+fp1(i,m)**2+sp1(i,m)**2)**2
      rL2=(eps+fp2(i,m)**2+sp2(i,m)**2)**2
      rL3=(eps+fp3(i,m)**2+sp3(i,m)**2)**2
      rR1=(eps+fm1(i,m)**2+sm1(i,m)**2)**2
      rR2=(eps+fm2(i,m)**2+sm2(i,m)**2)**2
      rR3=(eps+fm3(i,m)**2+sm3(i,m)**2)**2
      betaL1=CL1/rL1
      betaL2=CL2/rL2
      betaL3=CL3/rL3
      betaR1=CR1/rR1
      betaR2=CR2/rR2
      betaR3=CR3/rR3
      sumL=betaL1+betaL2+betaL3
      omegaL1=betaL1/sumL
      omegaL2=betaL2/sumL
      omegaL3=betaL3/sumL
      sumR=betaR1+betaR2+betaR3
      omegaR1=betaR1/sumR
      omegaR2=betaR2/sumR
      omegaR3=betaR3/sumR
      wfL(i,m)=omegaL1*fL1(i,m)+omegaL2*fL2(i,m)
     &                         +omegaL3*fL3(i,m)
      wfR(i,m)=omegaR1*fR1(i,m)+omegaR2*fR2(i,m)
     &                         +omegaR3*fR3(i,m)
 300  continue
      do 500 m=1,mm
      do 500 i=1,imax-1
      fn(i,m)=0.5d0*(wfL(i,m)+wfR(i+1,m))
 500  continue
      visc=0.0d-0/rho
c     do 544 m=1,mm
      do 544 i=2,imax-1
      dx=x_xi(i)*dxi
      rhs(i,1)=-(fn(i,1)-fn(i-1,1))/dx
      rhs(i,2)=-(fn(i,2)-fn(i-1,2))/dx
     $         -visc*q2(i)/q1(i)
 544  continue
      return
      end

ccccccccccccccccccccccccccccccccccc
cc    Original Explicit? Method
ccccccccccccccccccccccccccccccccccc
      subroutine res2
      implicit real*8(a-h,o-z)
      PARAMETER(nx=404,mm=2)
      COMMON /QQQQ/ Q1(-1:NX),Q2(-1:NX),Q3(-1:NX)
      COMMON /STEP/ DX,DT,CFL
      COMMON /NIJK/ IMAX
      common /pppp/ pmin
      common /block6/ ao(-1:nx),beta(-1:nx),YM(-1:nx)
      common /gggg/ x_xi(nx),dxi
      common /dddd/ cro,rho
      common /blk2/ rhs(nx,2)
      common /work1/ split,press,Fnp,Fnm
      common /work2/ fp1,fp2,fp3,sp1,sp2,sp3
      common /work3/ fm1,fm2,fm3,sm1,sm2,sm3
      common /work4/ fL1,fL2,fL3
      common /work5/ fR1,fR2,fR3
      common /work6/ wfL,wfR
      common /work7/ fn
      dimension split(-1:nx),press(-1:nx)
```

```
      dimension Fnp(-2:2,-1:nx,mm),Fnm(-2:2,-1:nx,mm)
      dimension fp1(-1:nx,mm),fp2(-1:nx,mm),fp3(-1:nx,mm)
      dimension sp1(-1:nx,mm),sp2(-1:nx,mm),sp3(-1:nx,mm)
      dimension fm1(-1:nx,mm),fm2(-1:nx,mm),fm3(-1:nx,mm)
      dimension sm1(-1:nx,mm),sm2(-1:nx,mm),sm3(-1:nx,mm)
      dimension fL1(-1:nx,mm),fL2(-1:nx,mm),fL3(-1:nx,mm)
      dimension fR1(-1:nx,mm),fR2(-1:nx,mm),fR3(-1:nx,mm)
      dimension wfL(-1:nx,mm),wfR(-1:nx,mm)
      dimension fn(-1:nx,mm)
      eps=1.d-6
      do 112 i=-1,imax+1
      A      = 0.5d0*(q1(i)+q1(i+1))
      bbeta  = 0.5d0*(beta(i)+beta(i+1))
      aao    = 0.5d0*(ao(i)+ao(i+1))
      dpda   = 0.5d0*bbeta/dsqrt(A)
      C      = dsqrt(A*dpda/rho)
      U      = 0
      split(i) = 1.0d0*(abs(u)+c)
 112  continue
ccc   flux splitting
      do 114 i=-1,imax+2
      A      = q1(i)
      bbeta  = beta(i)
      aao    = ao(i)
      p=bbeta*(dsqrt(A)-dsqrt(aao))+pmin
      press(i)= p
 114  continue
      do 120 i=1,imax-0
      do 120 j=-2,2
      A      = q1(i+j)
      U      = q2(i+j)
      bbeta  = beta(i+j)
      aao    = ao(i+j)
      p      = press(i+j)
      Fnp(j,i,1)  = U*A              +split(i)*A
      Fnp(j,i,2)  = 0.5d0*U*U+P/rho  +split(i)*U
      Fnm(j,i,1)  = U*A              -split(i-1)*A
      Fnm(j,i,2)  = 0.5d0*U*U+P/rho  -split(i-1)*U
 120  continue
ccc
      do 100 m=1,mm
      do 100 i=1,imax-0
      fp1(i,m)= 0.5d0*(fnp(-2,i,m)-4.d0*fnp(-1,i,m)+3.d0*fnp(0,i,m))
      fp2(i,m)= 0.5d0*(fnp( 1,i,m)-     fnp(-1,i,m)             )
      fp3(i,m)=-0.5d0*(fnp( 2,i,m)-4.d0*fnp( 1,i,m)+3.d0*fnp(0,i,m))

      sp1(i,m)= fnp(-2,i,m)-2.d0*fnp(-1,i,m)+fnp( 0,i,m)
      sp2(i,m)= fnp( 1,i,m)-2.d0*fnp( 0,i,m)+fnp(-1,i,m)
      sp3(i,m)= fnp( 2,i,m)-2.d0*fnp( 1,i,m)+fnp( 0,i,m)

      fm1(i,m)= 0.5d0*(fnm(-2,i,m)-4.d0*fnm(-1,i,m)+3.d0*fnm(0,i,m))
      fm2(i,m)= 0.5d0*(fnm( 1,i,m)-     fnm(-1,i,m)             )
      fm3(i,m)=-0.5d0*(fnm( 2,i,m)-4.d0*fnm( 1,i,m)+3.d0*fnm(0,i,m))

      sm1(i,m)= fnm(-2,i,m)-2.d0*fnm(-1,i,m)+fnm( 0,i,m)
      sm2(i,m)= fnm( 1,i,m)-2.d0*fnm( 0,i,m)+fnm(-1,i,m)
      sm3(i,m)= fnm( 2,i,m)-2.d0*fnm( 1,i,m)+fnm( 0,i,m)
 100  continue
      hh=0.5d0
      hh2=1.d0/8.d0
c     hh=0.0d0
c     hh2=0.d0/8.d0
      do 200 m=1,mm
      do 200 i=1,imax-0
      fL1(i,m)=fnp(0,i,m)+hh*fp1(i,m)+hh2*sp1(i,m)
      fL2(i,m)=fnp(0,i,m)+hh*fp2(i,m)+hh2*sp2(i,m)
      fL3(i,m)=fnp(0,i,m)+hh*fp3(i,m)+hh2*sp3(i,m)
      fR1(i,m)=fnm(0,i,m)-hh*fm1(i,m)+hh2*sm1(i,m)
      fR2(i,m)=fnm(0,i,m)-hh*fm2(i,m)+hh2*sm2(i,m)
      fR3(i,m)=fnm(0,i,m)-hh*fm3(i,m)+hh2*sm3(i,m)
 200  continue
      CL1=1.d0/16.d0
      CL2=10.d0/16.d0
      CL3=5.d0/16.d0
      CR1=5.d0/16.d0
      CR2=10.d0/16.d0
      CR3=1.d0/16.d0
      do 300 m=1,mm
      do 300 i=1,imax-0
      rL1=(eps+fp1(i,m)**2+sp1(i,m)**2)**2
      rL2=(eps+fp2(i,m)**2+sp2(i,m)**2)**2
```

```
      rL3=(eps+fp3(i,m)**2+sp3(i,m)**2)**2
      rR1=(eps+fm1(i,m)**2+sm1(i,m)**2)**2
      rR2=(eps+fm2(i,m)**2+sm2(i,m)**2)**2
      rR3=(eps+fm3(i,m)**2+sm3(i,m)**2)**2
      betaL1=CL1/rL1
      betaL2=CL2/rL2
      betaL3=CL3/rL3
      betaR1=CR1/rR1
      betaR2=CR2/rR2
      betaR3=CR3/rR3
      sumL=betaL1+betaL2+betaL3
      omegaL1=betaL1/sumL
      omegaL2=betaL2/sumL
      omegaL3=betaL3/sumL
      sumR=betaR1+betaR2+betaR3
      omegaR1=betaR1/sumR
      omegaR2=betaR2/sumR
      omegaR3=betaR3/sumR
      wfL(i,m)=omegaL1*fL1(i,m)+omegaL2*fL2(i,m)
     &                         +omegaL3*fL3(i,m)
      wfR(i,m)=omegaR1*fR1(i,m)+omegaR2*fR2(i,m)
     &                         +omegaR3*fR3(i,m)
 300  continue
      do 500 m=1,mm
      do 500 i=1,imax-1
      fn(i,m)=0.5d0*(wfL(i,m)+wfR(i+1,m))
 500  continue
      visc=0.0d-0/rho
c     do 544 m=1,mm
      do 544 i=2,imax-1
      dx=x_xi(i)*dxi
      rhs(i,1)=-(fn(i,1)-fn(i-1,1))/dx
      rhs(i,2)=-(fn(i,2)-fn(i-1,2))/dx
     $         -visc*q2(i)/q1(i)
 544  continue
      return
      end

      subroutine trids(a,b,c,d,n,nd)
      implicit real*8(a-h,o-z)
      dimension a(nd),b(nd),c(nd),d(nd)
      do 10 j=2,n
      aj=a(j)
      jj=j-1
      d(j)=d(j)-aj*d(jj)
 10   continue
      bn=b(n)
      d(n)=d(n)/bn
      do 30 j=n-1,1,-1
      jj=j+1
      bj=b(j)
      cj=c(j)
      d(j)=(d(j)-cj*d(jj))/bj
 30   continue
      return
      end
      subroutine tridf(a,b,c,n,nd)
      implicit real*8(a-h,o-z)
      dimension a(nd),b(nd),c(nd)
      do 10 j=2,n
      a(j)=a(j)/b(j-1)
      b(j)=b(j)-a(j)*c(j-1)
 10   continue
      return
      end


ccccccccccccccccccccccccccccccccccccccccccccc
ccc   setup time scale and BC's
ccccccccccccccccccccccccccccccccccccccccccccc
      subroutine calcBCs(istart,iend,dt)
      parameter(nt=100001,nx=404,ntshort=10001)
      IMPLICIT REAL*8(A-H,O-Z)
      common /block1/ x(nx),t(nt)
      common /block3/ pin(nt),uin(nt),ain(nt)
      common /block3a/ prr(nt),urr(nt),arr(nt)
      common /block6/ ao(-1:nx),beta(-1:nx),YM(-1:nx)
      common /block7/ cin(nt),crr(nt)
      common /dddd/ cro,rho
      common /pppp/ pmin
      common /ppp2/ pmax,tp
```

```
      common /nnnn/ npulse, n

c     write(*,*) 'calcBCs, istart=',istart,', iend=',iend

      pi=4.d0*datan(1.d0)

      do 20 i=istart,iend
       t(i-istart+1)=dt*(i-1)
 20   continue


cccc   boundary condition at j=1, right-running pulse with (pmin-pmax)
cccc   ap is wrong if alpha is not 1
      alpha=1.d0
      ap=(pmax-pmin)*dsqrt(2.d0)*dexp(alpha*pi/4.d0)
      alpha=0.d0
      ap=(pmax-pmin)
      tpt=npulse*tp

      do 14 i=1,iend-istart+1
       pin(i)=pmin
       ipulse=t(i)/tp+1
       if(ipulse.le.npulse) then
        if(t(i).lt.tpt) then
         tp1=1.d0*tp
         taw=pi*(t(i)-float(ipulse-1)*tp)/tp1
         if(taw.gt.pi) then
          pin(i)=pmin
         else
          taw1=0.25d0*taw/0.165d0
          if(taw1.gt.pi) taw1=pi
           pin(i)=pmin+ap*dexp(-alpha*taw)*dsin(taw1)
         end if
        end if
       end if
 14   continue

ccc   compute area corresponding to inflow pressure pulse
      aao=ao(1)
      bbeta=beta(1)
      aaa=ao(1)
      call pofa(ppp,aaa,dpda,aao,bbeta,-1)
      cro=dsqrt(aao*dpda/rho)
      do 114 i=1,iend-istart+1
       ppp=pin(i)
       call pofa(ppp,aaa,dpda,aao,bbeta,-1)
       cr=dsqrt(aaa*dpda/rho)
       ain(i)=aaa
       uin(i)=(pin(i)-pmin)/(rho*cr)
       cin(i)=cr
       uin(i)=4.d0*(cin(i)-cro)
 114  continue

cccc   boundary condition at j=n, left-running pulse with zero amplitude!!
      ap=0.d0
      aao=ao(n)
      bbeta=beta(n)
      aaa=ao(n)
      call pofa(ppp,aaa,dpda,aao,bbeta,-1)
      cro=dsqrt(aao*dpda/rho)
      do 16 i=1,iend-istart+1
       prr(i)=pmin
       ppp=prr(i)
       call pofa(ppp,aaa,dpda,aao,bbeta,-1)
       cr=dsqrt(aaa*dpda/rho)
       arr(i)=aaa
c      urr(i)=-(prr(i)-pmin)/(rho*cr)
       crr(i)=cr
       urr(i)=0.d0
 16   continue
      return
      END
ccccccccccccccccccccccccccccccccccccccccccccccccccc
```

Vita

John J. Charonko, III was born on October 8, 1979 in Martinsburg, West Virginia. At the age of five he moved to Charleston, West Virginia, where he remained until his graduation from George Washington High School in 1998. After graduation, John attended college at Virginia Tech in Blacksburg, Virginia, where he was awarded the Dan H. Pletta Award for Most Outstanding Senior Project. He graduated Summa Cum Laude in the Spring of 2002 and earned the degree of Bachelor of Science from the Department of Engineering Science and Mechanics, with minors in Computer Science and Mathematics. John remained at Virginia Tech for his Master's research, and is currently pursuing and Ph.D. in Biomedical Engineering. In addition to his primary research in computational modeling and cardiovascular fluid mechanics, his research has also included experimental work in flow control and the application of Digital Particle Image Velocimetry (DPIV) to a wide variety of experimental conditions. His hobbies and interests include downhill skiing, swing dancing, music, and computers.